UNIVERZITA PALACKÉHO V OLOMOUCI

Přírodovědecká fakulta

Katedra biochemie

Molekulární a funkční charakterizace embryonálního vývoje u dvojitých mutantů HSP90 a YODA

BAKALÁŘSKÁ PRÁCE

Autor:	**Natálie Závorková**
Studijní program:	B1406 Biochemie
Studijní obor:	Biotechnologie a genové inženýrství
Forma studia:	Prezenční
Vedoucí práce:	**Despina Samakovli, Ph.D.**
Rok:	2019

PALACKY UNIVERSITY OLOMOUC

Faculty of Science

Department of Biochemistry

Molecular and functional characterization of double mutants of HSP90 and YODA regarding embryogenesis

BACHELOR THESIS

Author:	**Natálie Závorková**
Study programme:	B1406 Biochemistry
Field of study:	Biotechnology and Gene Engineering
Form of study:	Full
Supervisor:	**Despina Samakovli, Ph.D.**
Year:	2019

Prohlašuji, že jsem bakalářskou práci vypracovala samostatně s vyznačením všech použitých pramenů a spoluautorství. Souhlasím se zveřejněním bakalářské práce podle zákona č. 111/1998 Sb., o vysokých školách, ve znění pozdějších předpisů. Byla jsem seznámena s tím, že se na moji práci vztahují práva a povinnosti vyplývající ze zákona č. 121/2000 Sb., autorský zákon, ve znění pozdějších předpisů.

V Olomouci dne ..... ……...

I declare that I developed this bachelor thesis separately with showing all the sources and authorship. I agree with the publication of the thesis by Act no. 111/1998 Coll., about universities, as amended. I was awared of that the rights and obligations arising from the Act no. 121/2000 Coll., the Copyright Act, as amended, are applied to my work.

At Olomouc …… ……...……

Poděkování

nejprve bych chtěla upřímně poděkovat své vedoucí Despině Samakovli, za její nesmírnou trpělivost, odborné rady a ochotu vysvětlit příčinu nezdarů nebo diskuzi u výsledků. Také jí děkuji za podporu v rámci studia, pomoc při bourání jazykových bariér a rozšíření jazykových znalostí. Dále bych chtěla poděkovat Terce Tiché a Terce Vavrdové za vysvětlení nových laboratorních postupů, ochotu pomoct a hlavně přijetí do laboratorního týmu. Terce Tiché děkuji za ochotu naučit mě mimo jiné Western blotting a Terce Vavrdové za objasnění mikroskopických technik. Všem třem inteligentním ženám děkuji za předání nadšení pro vědu a zvláště pro rostliny. Nakonec bych chtěla poděkovat celému oddělení buněčné biologie za skvělé pracovní prostředí.

Acknowledgements

First of all, I would like to sincerely thank my supervisor Dr. Despina Samakovli for her immense patience, expert advice and willingness to explain the cause of the failures or discussion of the results. I would also like to thank her for her support during my studies and help with breaking language barriers. Furthermore, I would like to thank Terka Tichá and Terka Vavrdová for explaining new laboratory procedures, willingness to help and mainly for accepting me in the laboratory team. Terka Tichá, thank you for your willingness to teach me, among other things, Western blotting and Terka Vavrdová, thank you for clarifying microscopic techniques. My thanks belong to these three intelligent women for enhancing my passion for science and especially for plants. Finally, I would like to thank the whole department of cell biology for great working environment.

Bibliografická identifikace

Jméno a příjmení autora	Natálie Závorková
Název práce	Molekulární a funkční charakterizace embryonálního vývoje u dvojitých mutantů HSP90 a YODA
Typ práce	Bakalářská
Pracoviště	Katedra biochemie
Vedoucí práce	Despina Samakovli, Ph.D.
Rok obhajoby práce	2019

Abstrakt

Tato bakalářská práce se zaměřuje na vliv YODA-MAPK kaskády a HSP90 na embryonální vývoj rostliny. Fenotypově i molekulárně byly charakterizovány vlivy jednotlivých komponentů signální dráhy, jmenovitě YDA, MPK3, MPK6, HSP90.1 a HSP90.3, na ranou embryogenezi, vývoj primárního kořene semenáčků a vývoj reprodukčních orgánů rostliny.

Správný vývoj embrya je nezbytný pro celkový vývoj organismu. Defekty v embryogenezi mohou mít dalekosáhlé a nevratné následky v průběhu celého životního cyklu rostliny. Proto je důležité pochopit vývojový model rané embryogeneze. Je známo, že YDA-MAPK kaskáda se podílí na asymetrických buněčných děleních, které řídí vývoj stomat a podílí se na prvním asymetrickém dělení zygoty při embryogenezi. Dalším již publikovaným faktem je ovlivnění výše zmíněné signální dráhy HSP90 v rámci procesu tvorby stomat. Hlavním cílem této práce bylo zjistit, zda i v rámci raného embryonálního vývoje jsou tyto dva komponenty v interakci a zda oba ovlivňují embryogenezi v rámci jedné molekulární dráhy. Tohoto cíle bylo dosaženo zkoumáním jednoduchých a dvojitých mutantů členů YODA-MAPK kaskády a HSP90. Výsledky jednotlivých experimentů naznačují, že je YODA-MAPK kaskáda opravdu ovlivňována proteiny z rodiny HSP90.

Klíčová slova	Heat shock protein 90, MPK3, MPK6, raná embryogeneze, YDA YODA-MAPK signální dráha, WOX8,
Počet stran	80
Počet příloh	0
Jazyk	Anglický (Český)

Bibliographical identification

Autor's first name and surname	Natálie Závorková
Title	Molecular and functional characterization of double mutants of HSP90 and YODA regarding embryogenesis
Type of thesis	Bachelor
Department	Department of biochemistry
Supervisor	Despina Samakovli, Ph.D.
The year of presentation	2019

Abstract

This bachelor thesis focused on the influence of YODA-MAPK cascade and HSP90 on the embryonic development of the plant. The phenotypic and molecular characterization of the individual components of the signaling pathway, namely YDA, MPK3, MPK6, HSP90.1 and HSP90.3, on early embryogenesis, development of primary root of seedling and development of plant reproductive organs were characterized.

The proper embryonic development is essential for correct development of the organism. Defects in embryogenesis may have far-reaching and irreversible consequences for the continuation of the plant's life cycle. Therefore, it is important to understand the developmental pattern of early embryos. It is known that the YODA-MAPK cascade is involved in asymmetric cell divisions that control stomatal development and contribute to the first asymmetric division of a zygote in embryogenesis. Another already published fact is the influence of the HSP90 on the above-mentioned signaling pathway in the process of stomatal formation. The main aim of this work was to investigate whether these two components are in interaction even during the early embryonic development and whether they both influence embryogenesis within one molecular pathway. This goal was achieved by examining single and double mutants of the members of YODA-MAPK cascade and HSP90 protein family. The results of individual experiments suggest that the YODA-MAPK cascade is indeed influenced by proteins from the HSP90 family.

Keywords	early embryogenesis, Heat shock protein 90, MPK3, MPK6, YDA, YODA-MAPK cascade, WOX8
Number of pages	80
Number of appendices	0
Language	English (Czech)

Content

Aims of the bachelor thesis

Theoretical part

In theoretical part I summarize existing knowledge about embryonic development of *Arabidopsis thaliana*, mitogen-activated protein kinases and their involvement in signal transduction by MAPK-cascades and furthermore, a review of heat shock proteins focusing on the HSP90 protein family.

Experimental part

The first goal is the phenotypic and functional characterization of single and double mutants and their comparison. In the thesis I focused on the length of seedling roots, flower development and the early stages of embryogenesis in single mutants, such as Δ*Nyda*, *yda*, *mpk3, mpk6, hsp90.1, hsp90.3* and *pRac2::hsp90RNAi* and double mutants, such as *hsp90.1*Δ*Nyda*, *hsp90.1yda, hsp90.3*Δ*Nyda* and *hsp90.3yda*. Furthermore, I studied abundance of both phosphorylated and unphosphorylated forms of MPK3 and MPK6 and abundance of HSP90 proteins in *mpk3, mpk6, hsp90.1, hsp90.3* single mutants and *pRac2::hsp90RNAi* line by western blotting analysis.

The second goal is molecular characterisation of single and double mutants. For this purpose, we crossed Δ*Nyda*, *yda*, *mpk3-1, mpk6-2, hsp90.1* and *hsp90.3* mutant lines with pWOX8::NSL:YFP reporter line. The produced mutant lines with pWOX8::YFP reporter were selected by genotyping and characterized by microscopic observations.

1 Introduction

A. thaliana is widely used as a model organism in modern plant science due to several traits. Current research is focused on the function of individual genes, their products (proteins) and the relationships between them.

The proper embryonic development is essential for correct development of the organism. Defects in embryogenesis may have far-reaching and irreversible consequences for the continuation of the plant's life cycle. Therefore, it is important to understand the developmental pattern of early embryos. During embryogenesis process, the first polar division of zygote is regulated by a MAPK-signaling pathway.

Mitogen activated protein kinases (MAPKs) are ubiquitous proteins. Proteins of this class are divided into three subclasses, which are strictly hierarchically ordered. MAPKs are activated by MAPKKs (mitogen activated protein kinase kinase), which are regulated by MAPKKKs (mitogen activated protein kinase kinase kinase). It is known, that YODA-MAPK cascade is involved in asymmetric cell divisions, which control stomata development, while YODA-MAPK signaling cascade (YDA-MAPKK4/5-MPK3/6; Meng et al., 2012) is involved in the division of zygote (Lukowitz et al., 2004).

Another topic I am dealing with in the bachelor thesis are heat shock proteins 90 (HSP90). HSP90s are essential for cell viability under ideal conditions and even under stress conditions. The primary function of heat shock proteins is protein folding. Being called molecular chaperones, they assist the formation of tertiary and quaternary structure of other proteins regulating protein accumulation and localization. HSPs are divided into 5 groups according to molecular weight. *Arabidopsis thaliana* carries in its genome genes for 7 proteins belonging to the HSP90 group (Krishna and Gloor, 2001). My bachelor thesis focused on HSP90.1 and HSP90.3 and their presumptive interaction with YODA-MAPK cascade.

Last part of the thesis deals with WOX8 (WUSCHEL HOMEOBOX 8). WOX8 is a transcription factor from the WUSCHEL family. Its expression is controlled among others by YODA-MPK cascade. WOX8 is typically expressed in the cells of the suspensor during embryogenesis and it is considered a main regulator of early embryonic development (Ueda *et al.,* 2017).

2 Current State of the Topic

2.1 *Arabisopsis thaliana* (Mouse-ear cress)

Arabidopsis thaliana is a dicotyledonous plant. It is a member of the *Brassicaceae* family which includes also agriculturally important crops (for example cabbage or radish). The distribution of the plant is nearly worldwide, especially in temperate and sub-tropical zone of the Northern Hemisphere.

A. thaliana is now widely used as a model organism in modern plant science due to several traits. *Arabidopsis* is a small plant, which can be easily cultivated in quantity in cultivation rooms, growth chambers or greenhouses. Another advantage is the short life cycle of the plant, enabling to harvest abundance of seeds several times a year. Furthermore, it is a self-pollinated plant and has small genome that is advantageous.

A. thaliana has five chromosomes and the total length of the genomic DNA is approximately 135 Mb. In *Arabidopsis*, sophisticated methods of gene manipulation have been developed, for instance, protocols for efficient stable transformation with *Agrobacterium tumefaciens*. There are centres stockpiling thousands of *A. thaliana* mutant lines and ecotypes, which collaborate with research centres (e.g. TAIR: https://www.arabidopsis.org/portals/education/aboutarabidopsis.jsp (27.8.2018); GABI-Kat https://www.gabi-kat.de/ 11.9.2018).

Arabidopsis thaliana was discovered by Johannes Thal, in whose honour the plant was named, in the Harz Mountains (Germany) in the sixteenth century. In the first half of the 20th century, German botanist Friedrich Laibach, together with his student Erna Reinholz, began to explore the potential use of *A. thaliana* as a model organism. In the 1980s, the use of *A. thaliana* for the study of plant physiology, biochemistry and developmental biology expanded. The first functional transformation using *Agrobacterium* was published in 1986 (Meyerowitz, 2001).

In 1990, the Arabidopsis Genome Project was initiated, and by 2000 the genome was completely sequenced. Current research is focused on the function of individual genes, their products and the relationships between them. While it may seem that almost everything is known about this small plant, *Arabidopsis thaliana* is still surrounded with mystery.

2.2 Embryogenesis

The proper embryonic development is essential for the correct development of the organism. Defects in embryogenesis may have far-reaching and irreversible consequences for the continuation of the plant's life cycle. Therefore, it is important to understand the developmental pattern of early embryos.

Double fertilization is typical for the plant kingdom. Pollen grains contain three nuclei: one diploid and two haploids. The diploid nucleus, called vegetative, regulates the cellular functions of the pollen and the two haploid nuclei, called generative, serve for reproduction (Peris et al., 2010). After a pollen tube penetrates to the inner space of the embryo sac, one generative nucleus merges with the central cell (diploid) to form the endosperm (triploid). The second generative nucleus merges with the egg cell to form the zygote (diploid; Peris et al., 2010).

Prior to fertilization, the egg cell is polarized in the direction of the micropyle. After fertilization of the egg cell, the nucleus travels to the central part and the vacuole is divided into smaller parts that are evenly dispersed. After a short non-polar phase, the cell repolarizes. (Jeong *et al*., 2016).

The process of controlled elongation, including polarization, is not completely understood, however, it is certain that several polarization factors are involved. Many of these factors are not discovered yet. Nevertheless, one of the known substances is auxin. This hormone is essential for apical/basal meristem growth, elongation of main and lateral roots or leaflet development (Peris et al., 2010).

ROP (RHO GTPase OF PLANT) plays an important role in polarization of the actin cytoskeleton and the position of the cell plate in dividing cells during embryogenesis (Huang et al., 2014).

Signalling pathway involving MAPKKK YODA participates in the formation of the apical-basal axis of the zygote, which will be further discussed in detail in the chapter dealing with the YODA-MAPK cascade.

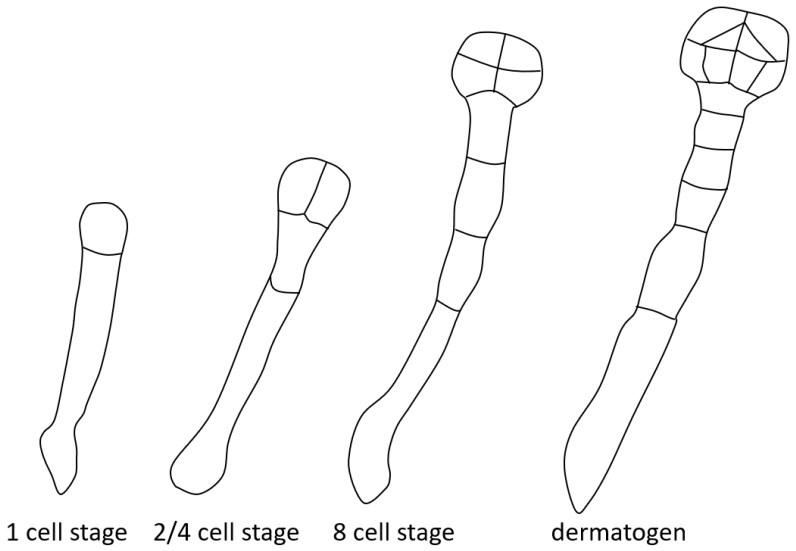

Figure 1: Early embryogenesis of *Arabidopsis thaliana*.

The prolonged zygote cell is divided asymmetrically into two cells - apical and basal. The apical cell is significantly smaller, its cytoplasm is denser and contains a non-visible vacuole. Further divisions in apical cells lead to the formation of the embryo. The basal cell is directed towards the micropylar pole and compared to the apical cell it is longer and vacuolized.

The transversely dividing basal cell produces a fibrous formation - the suspensor (Bayer et al., 2017). The suspensor has two main functions. The first function of the suspensor is to link the embryo to the embryonic-sac to support the nutrition supply. The second function of the suspensor is to maintain the embryo in the endosperm space. The suspensor is divided transversally, and the number of cells is unique for each developmental stage of the embryo (Lukowitz et al., 2004).

The apical cell, in contrast to the basal cell, divides twice longitudinally into a four-cell embryo. This is followed by transversal division to an eight-cell embryo. After that, the embryo is visibly separated into the upper layer and lower layer. Both layers undergo periclinal division while an outer layer of cells (protoderm) is established. At this stage, a typical pentagonal cell formation is distinguishable by microscopic observation. The stage of embryogenesis is called dermatogen (Figure 1; Bayer et al., 2017).

Further divisions result in the formation of a globular embryo (globular stage) during which the differentiation can be already observed. Continuous divisions occur through transient (triangular) stage to heart stage and subsequently to torpedo stage. In

the latter stages, the rudiments are already established for all types of tissues including the primary root vascular tissues, the apical meristem and cotyledons (Boscá *et al*. 2011; Lau et al., 2012).

The preceding paragraphs described the division of cells leading to the formation of a strictly defined pattern. An important feature of cell divisions is regularity. Each division is precisely programmed and only its proper implementation leads to the formation of a functional embryo. Even small mistakes or deviations from the evolutionally preserved system may result in significant defects. The changes compared to normal early development of the embryo will be reflected in subsequent development. The more prominent the changes are, the more pronounced the resulting phenotype of the plant will be (Bayer *et al*. 2017).

Finally, the embryo enters dormancy which acts as a temporary stop or a significant slowdown in all biochemical and physiological processes. This helps seeds to survive the winter. And when the conditions are appropriate the seed initiates germination, and the embryo develops to a seedling (Bayer *et al*. 2017; ten Hove *et al*. 2015).

2.3 Mitogen activated protein kinases

Mitogen activated protein kinases (MAPKs) are ubiquitous proteins, components of wide range of life-essential processes. Proteins of this class are divided into three subclasses, which are strictly hierarchically ordered. MAPKs are activated by MAPKKs (MAP2K; mitogen activated protein kinase kinase), which are regulated by MAPKKKs (MAP3K; mitogen activated protein kinase kinase kinase). Thus, organized MAPK signaling pathways play a crucial role in the development and survival of an organism.

This chapter discusses the classification and function of MAPKs. MAPKs are enzymes belonging to the transferase family. Transferases catalyze chemical reactions in which the functional group is transferred from the donor molecule to the acceptor molecule. Transferases include kinases, but also aminotransferases, transaldolases, transketolases and others. Kinases transfer a phosphate group from a high-energy donor molecule (typically ATP) to a target molecule (substrate) in a process called phosphorylation. The reverse process (dephosphorylation) is catalyzed by phosphatases (Kodíček *et al.,* 2018).

Protein kinases transfer the phosphate group to the protein to form a phosphoester bond. Phosphate binds to the hydroxyl group of the side chains of amino acids. Depending on the type of phosphorylated group, kinases are divided into (1) serine / threonine kinases (including MAPKs) and (2) tyrosine kinases (Ichimura *et al*., 2002).

Formation of signalling cascades is typical for MAPKs. Cascade is a hierarchically structured system in which each biochemical reaction is connected. Each of this reaction is catalysed by different cascade kinase and is regulated by the previous reaction, along with controlling the following reaction. External conditions stimulate cell membrane receptors, sometimes called MAPKKKKs, thereby MAPK cascade is activated (Colcombert and Hirt, 2008; Rodriguez et al., 2010). The MAPK cascade itself is triggered by a phosphorylation of the serine/threonine MAPKKK. This MAPKKK phosphorylates dual-specific MAPKK at the serine or threonine site in a preserved S/T-X_{3-5}-S/T motif (Serine/Threonine- X_{3-5}- Serine/Threonine). Signal pathway ends with MAPK dual phosphorylation. Dual phosphorylation is the simultaneous phosphorylation of two MAPK amino acids on the T-X-Y motif (Threonine-X-Tyrosine), which is phosphorylated by only one MAPKK (Colcombert and Hirt, 2008; Rodriguez et al., 2010; figure 2).

The advantage of continuity of the cascade is the possibility of relatively easy and fast transmission of signal or information. The cascade can be very effectively regulated. Genome of *A. thaliana* contains genes encoding about 60-80 MAPKKKs, 10 MAPKKs and 20 MAPKs. The ratio of MAPKK to MAPK suggests that one MAPKK may activate multiple MAPKs (Ichimura K. *et al.*, 2002). The signaling

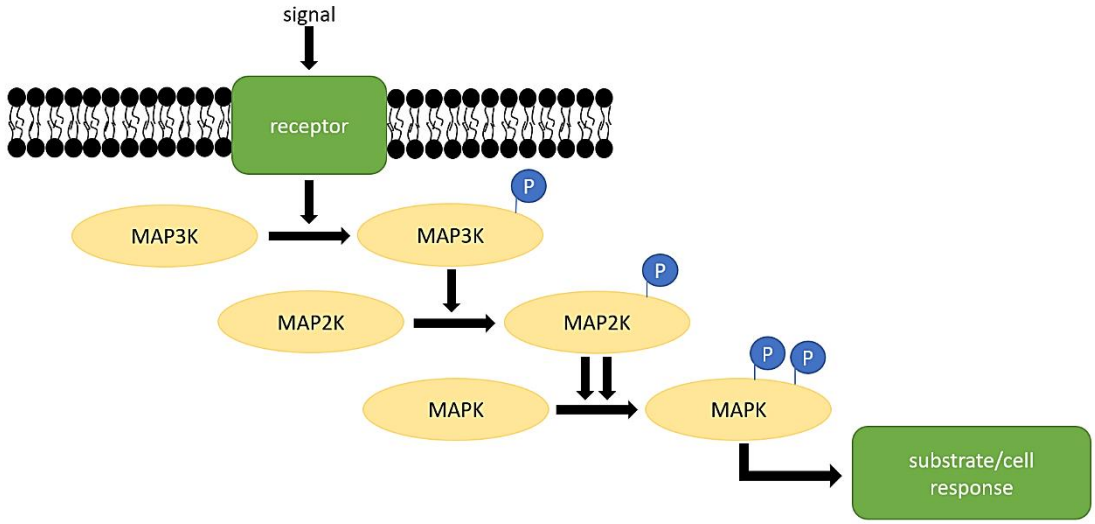

Figure 2: Model of MAPK signaling pathway

pathways are interconnected (cross-talk), therefore one stimulus can lead to a complex response of the cell, tissue or organism. On the contrary, numerous different stimuli can lead to one response, which is beneficial in these conditions. Individual kinases may be involved in several different signaling pathways, thus influencing various physiological processes (Ichimura et al., 2002; Colombert and Hirt, 2008).

Inactivation of the signalling pathway is regulated by Serine/Threonine or Tyrosine specific phosphatases. These enzymes catalyse dephosphorylation of amino acids on the active site of MAPKs (Rodriguez *et al.*, 2010). Another mechanism of MAPK cascade regulation is by scaffold proteins that bind two or more signaling pathway molecules. These proteins can facilitate the clustering of individual members of the signaling pathways and sequester them in a certain cell space or prevent the MAPKs from inactivation (Meister et al., 2013).

2.3.1 Plant MAPK cascades

The first kinase family in hierarchy, MAPKKK, is divided into two subfamilies: (1) MEKK-like kinases, which are similar to mammalian MEKK1 (mammalian MAP/ERK kinase kinase 1). This subfamily including MEKK1, MEKK2 and YODA (Virk *et al.*, 2015; Smékalová *et al.*, 2014). (2) RAF-like kinases (rapidly accelerated fibrosarcoma) including CTR1 (CONSTITUTIVE TRIPLE RESPONSE 1, Huang *et al.*, 2003) and EDR1 (ENHANCED DISEASE RESISTANCE 1, Zhao *et al.*, 2014).

The structure of MAPKKKs is characterised by its long N- or C- terminal domain, that facilitates regulation and/or binding to another MAPKs (Colcombet a Hirt, 2008).

MAPKKs, involved in the second step of the MAPK signalling cascade, are divided into four groups. The amino acid sequence of the phosphorylation motif is highly conserved in the S/T-X_{3-5}-S/T form (Serine/Threonine - five variable amino acids - Serine/Threonine; Ichimura K. *et al.*, 2002).

Mitogen activated protein kinases (MAPKs or MPKs) are the last step in the MAPK signaling pathway. MAPKs are divided into four groups (A-D), same as MAPKKs. The phosphorylation motif of plant MAPK includes three amino acids. Groups A-C comprise the same T-E-Y (Threonine-Glutamate-Tyrosine) motif, whereas MAPKs in group D have an amino acid sequence of T-D-Y (Threonine-Aspartate-Tyrosine) at their active sites. (Ichimura K. *et al.*, 2002)

Group A includes MPK3, MPK6 and MPK10. Transcription of MPK3 and MPK6 is activated by various environmental stress conditions (Ichimura K. et al., 2000), for

example by oxidative stress (Kovtun Y. et al., 2000). Both MPK3 and MPK6 are involved in cell response to the pathogen downstream to pathogen-associated molecular patterns (PAMPs; Devendrakumar *et al*., 2018). Furthermore, MPK6 plays an essential role in cell division by establishment of cell division plane, particularly in the formation of a pre-prophase band and phragmoplast (Müller *et al.*, 2010; Komis *et al*., 2018).

Among the members of MAPK group B are MPK4, MPK5, MPK11, MPK12 and MPK13 (Petersen et al., 2000). MPK4 belongs to the cascade induced in response to both biotic and abiotic stress (Ichimura et al., 2000).

Groups C and D contain fewer known kinases such as MPK7 (C) and MPK8 or MPK9 (D; Ichimura *et al*., 2002).

2.3.2 Function of MAPK cascades

MAPK signaling pathways play role in significant biological mechanisms, examples of which are mentioned in Figure 3. They are an important part of the cell cycle for regulating cell growth, division, differentiation, and programming cell death (Meng et al., 2012). They also participate in the development of the embryo (Lukowitz et al., 2004) and subsequent seedling growth and development through whole plant life (Komis *et al*., 2018). Another process regulated by MAPK is stomatal development and patterning (Bergmann et al., 2004; Gudesblat et al., 2012). Lastly, the MAPK cascade is involved on responses to stress conditions (Teige et al., 2004, Šamajová et al., 2013; Virk et al., 2015) and hormonal signaling (Smékalová et al., 2014).

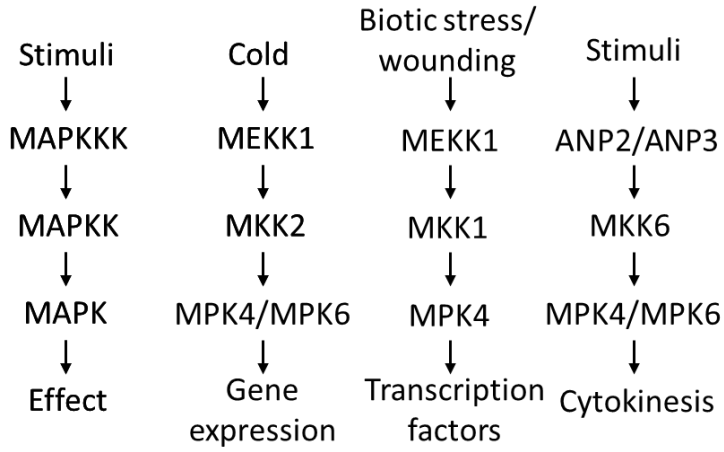

Figure 3: Scheme involving the presence of MAPK cascades in responses to both abiotic and biotic stress as well as other stimuli. This figure indicates the crosstalk of cascades - the presence of one MAPKKK (MEKK1) that phosphorylates two different MAPKKs; the same MAPK (MPK4) is phosphorylated by various MAPKKs.

2.3.3 The role of plant MAPK cascades in cytokinesis

During plant cell division, specific cytoskeletal structures are formed - preprophase ring, spindle, phragmoplast and cell plate (Müller, 2012; Komis *et al*., 2018). The correct orientation of the cell wall is a prerequisite for both the normal process of cytokinesis and the correct formation of plant tissues. In plants, two MAPK cascades were identified involved in the cell division.

The first cascade is composed of ANP2/3 (*Arabidopsis* homologue of Nucleus and Phragmoplast localized kinase family) - MKK6 - MPK4/6 (Takahashi *et al*., 2010). This cascade was first described in tobacco (*Nicotiana*) and alfalfa (*Medicago*; Calderini *et al*., 1998). The cascade is involved in the formation and expansion of the phragmoplast from the center of the cell to the dividing cell wall (Takahashi et al., 2010).

The second cascade is the YODA-MPK cascade (YDA, MAPKKK), comprised of YODA - MKK4/5 - MPK3/6 (Meng et al., 2012; Komis *et al*., 2018).

2.3.4 YODA-MAPK cascade

This chapter will discuss functions of signaling pathway, starting with the YODA kinase (Figure 4). An important property of YODA is the presence of the regulatory sequence in the N-terminal region. By interrupting this region, the YDA protein becomes constitutively active (so-called *ΔNyda*). Conversely, insertion of T-DNA into

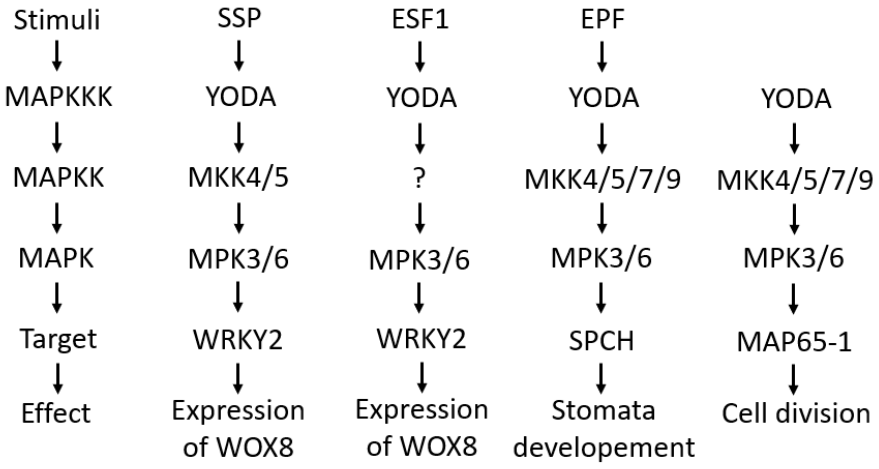

Figure 4: MAPK signaling cascades involving YDA MAP3K upstream of MPK3 and MPK6

the YODA gene (*yda* mutants) disrupts the reading frame. Therefore, the gene is not expressed and hence not translated into a functional protein (Lukowitz *et al.*, 2004).

The YODA-MAPK cascade is involved in cell division, for example in root growth. Mutant plants *yda* and *ΔNyda* exhibited significantly shorter length of the primary roots of the seedling and the defective establishment of cell division plane (Smékalová *et al*., 2014).

The YDA signalling pathway has an essential influence on stomatal patterning. Through regulation of SPCH (SPEECHLESS) transcription factor, the cascade regulates the initiation of stomatal development, by promoting the first asymmetric cell division (Komis *et al*., 2018). Phenotype of *yda* mutants exhibits a cluster of stomata in epidermis of the leaves. On the other hand, upregulation of YDA gene (Δ*Nyda* mutants) leads to stomata-less phenotype (Bergmann *et al*., 2004). Two of the MPKs downstream of YDA, namely MPK3 and MPK6, were also studied regarding stomatal development. Knockout mutants *mpk3* and *mpk6* exhibit abnormal stomatal clustering and defects in one-cell spacing rule, which indicate that MPK3 and MPK6 are negative regulators of stomatal development (Wang et al., 2007).

Furthermore, polarization of zygote, first asymmetric division and subsequent embryonic development are also affected by YDA cascade (Wang et al., 2007; Komis *et al*., 2018). Mutants *yda, mpk3* and *mpk6* exhibit embryonic developmental defects of both the suspensor and the embryo. Suspensor of *yda* mutant is shorter than the suspensor of wild type embryo and is often poorly recognizable. Furthermore, in *yda* mutant suspensor longitudinal division may occur instead of transversal divisions. At least one atypical division occurs in the two-fifths of cases (Lukowitz et al., 2004).

Transgenic plants with constitutively active YODA kinase (*ΔNyda* mutants) exhibit the opposite phenotype of development of the suspensor in embryonic development. More frequent cell divisions of the embryonic suspensor occur in the *ΔNyda* mutants than in the wild type. Moreover, the development of *ΔNyda* embryo is suppressed at the expense of the suspensor. The embryo in this case is smaller in comparison to the wild-type embryo. (Lukowitz *et al.*, 2004)

The YDA-MAPK cascade plays a crucial role in the polarization of the zygote and the first asymmetric division (Lukowitz *et al*., 2004). Although the regulation of the YDA-MAPK cascade has not yet been fully elucidated, there are some known proteins affecting the signaling pathway (figure 5 and figure 6).

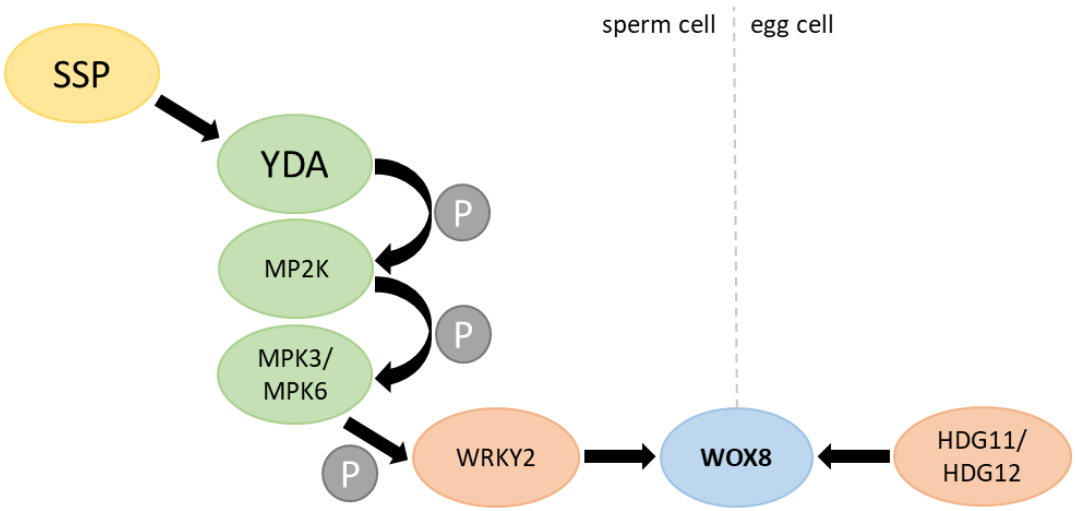

Figure 5: Model of signaling pathways leading to assymetry and elongation of zygote through WOX8 expression. Left part is showing sperm cells derived signal (SSP) and YODA-MAPK signaling cascade, witch activate WOX8 transcription through phosphorylation of WRKY2 transcription factor. Right part showes egg cell determined WOX8 transcription. Figure is based on Ueda *et al.*, 2017.

The first regulator belongs to the family of the cysteine-rich peptide EMBRYO SURROUNDING FACTORS (ESFs). These upstream regulators are secreted by the endosperm and support the formation of the apical-basal axis and promote the elongation of the suspensor (Costa *et al*., 2014).

Another regulator of the YDA-MAPK cascade is SHORT SUSPENSOR (SSP) that is receptor-like cytoplasmic kinase. SSP is present in the form of transcripts (mRNA) only in pollen sperm cells which are translated in zygotes after fertilization. The mechanism during which a protein (transcription factor) occurs only in one of the parental organisms is called parent-of-origin (Bayer *et al*., 2009). The phenotype of *ssp* mutants is less strong than the phenotype of *yda* mutants, indicating that YDA is regulated by multiple factors.

The YODA-MAPK cascade probably regulates a variety of proteins, especially transcription factors. At present, possibly the best investigated regulation by this cascade is the activation of the WRKY2 (*Arabidopsis thaliana* WRKY DNA-binding factor 2) transcription factor by this cascade. Zinc finger transcription factor WRKY2 positively regulates the expression of the WOX8 transcription factor. WOX8 belongs to the WUSCHEL transcription factors family, and it is expressed in the cells of the suspensor. It is the main regulator of early embryonic development (Ueda *et al.*, 2017).

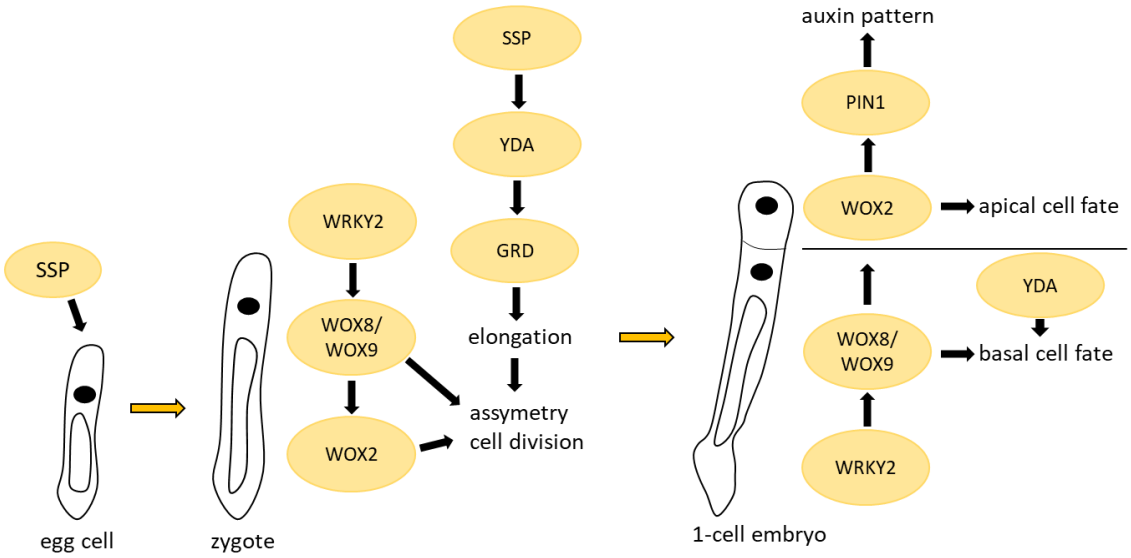

Figure 6: Model of establishing apical and basal cell fate during early embryogenesis. Sheme is showing gene/protein interactions and role of proteins in polar division and formation of embryo (apical cell fate) and suspensor (basal cell fate). Figure is based on Boscá *et al*., 2011.

The *wrky2* mutation leading to a non-functional transcription factor, is phenotypically manifested during asymmetric first division (Ueda *et al*., 2011).

Polarity and elongation of zygote are controlled via WOX8 by at least two pathways (figure 5). Firstly, by the paternally regulated YODA-MAPK cascade and secondly, by maternal factors, specifically with the aid of transcription factors HDG11 and HDG12 (HOMEODOMAIN GLABROUS). Both transcription factors WRKY2 and HDG11/12 directly bind to the WOX8 gene regulatory sequence leading to the initiation of its expression (Ueda *et al*., 2017).

2.4 Heat shock proteins

Heat shock proteins (HSPs) are essential for cell viability under both ideal conditions and stress. Due to the large number of HSP families, this chapter will focus on the HSP90 plant protein family.

HSPs were first described in the reaction of the organism to heat stress, which is why they were named heat shock proteins. Italian scientist Ferruccio Ritossa examined gene expression in *Drosophila melanogaster* after exposure to heat stress. This research is considered to be the first step to discovering HSPs (Ritossa, 1962). Subsequently, these proteins were identified and named as HSPs. (Tissieres *et al.*, 1974).

Heat shock proteins have been identified in almost all organisms. HSP analogs occur both in prokaryotic and eukaryotic organisms.

2.4.1 Function of heat shock proteins

The primary function of HSPs is protein folding. Being called molecular chaperones, they assist the formation of tertiary and quaternary structure of other proteins that regulate protein accumulation and localization. They are essential for the proper function of the cell and therefore, the whole organism (Feder and Hofmann, 1999; Panaretou and Zhai, 2008; Hu *et al*., 2009).

In response to stress, chaperone function is manifested by binding to a hydrophobic residue on the surface of proteins to prevent degradation (Panaretou et al., 1998), to assist re-folding of proteins upon damage and proper folding of newly translated proteins (Sharma *et al*., 2010; Mashaghi *et al*., 2016). Some HSPs, especially of smaller size, function as cochaperones. Smaller HSPs bind with other HSPs (chaperones) and help them function properly (Hartl 1996).

HSPs are also involved in signaling. For example, HSP70 regulates the activity of target proteins (Sharma *et al*., 2010; Mashaghi *et al*., 2016). Another example of HSP function is the suppression of apoptosis. For example, HSP70 in normal conditions binds to Apaf1 (Apoptotic protease activating factor 1). This blocks the formation of an apoptotic complex (apoptosome), which is important in the apoptosis process (Beere *et al*., 2000).

2.4.2 Heat shock protein families

Heat shock proteins are divided into families according to their molecular weights. This is reflected in the names of families. HSPs consists of five families: small HSP, HSP60, HSP70, HSP90 and HSP100 (Schlesinger, 1990, Kotak *et al*., 2007).

2.4.2.1 Small HSPs

Small HSPs have the lowest relative molecular weight (15-45 kDa) within the HSP group. These small proteins are characterized by α-crystalline domain and their function is not ATP-dependent (Waters, 2013). Small HSPs are the most abundant HSP family in a cell (Sun *et al*. 2001). In *Arabidopsis thaliana* there are 19 proteins belonging to this group (Scharf *et al*., 2001; Waters, 2013).

2.4.2.2 HSP60

HSP60 are specifically localized in mitochondria, however they can be also found in cytoplasm or other organelles (Kirchhoff *et al*., 2002; Balczun *et al*., 2006). They are only active when in complex with other HSPs (Hartl 1996). In conjunction with cochaperones from other HSP families, HSP60s transport proteins from the cytoplasm into the mitochondria (Bukau and Horwich 1998). Other functions of HSP60 in mitochondria are their involvement in replication (Kaufman *et al*., 2000) and the transfer of mitochondrial DNA to daughter cells (Kaufman *et al*., 2003).

2.4.2.3 HSP70

HSP70 is a highly researched group of proteins. HSP70s are essential for expression of other HSPs. Their expression is dependent on light-induced chloroplast signaling and HSF (heat shock factor, Dickinson *et al*., 2018). Similarly to HSP60, the chaperone function HSP70 often depends on the formation of HSP70 complexes with other HSPs (Kampinga and Craig, 2010).

2.4.2.4 HSP90

This group of heat shock proteins is the most relevant for this bachelor thesis, therefore this family will be discussed in more details, with a special emphasis on the proteins of the *Arabidopsis thaliana*. The subchapters focus on the characteristics of cytoplasmic HPS90 and their function in embryonic development.

Arabidopsis thaliana carries in its genome genes for 7 proteins belonging to the HSP90 group (Krishna and Gloor, 2001). They are further divided into two subgroups. The first subgroup consists of cytoplasmic HSP90, which are HSP90.1 (formerly HSP81.1), HSP90.2 (formerly HSP81.2), HSP90.3 (formerly HSP81.3), and HSP90.4 (formerly HSP81.4) proteins. The other three heat shock proteins, HSP90.5 (formerly HSP88.1), HSP90.6 (formerly HSP89.1), and HSP90.7 are found in chloroplasts, mitochondria, peroxisomes, or endoplasmic reticulum (Milioni and Hatzopoulos, 1997; Krishna and Gloor, 2001).

HSP90s are characterized by a conserved N-terminal (NTD) and C-terminal domain (CTD) and a more variable middle domain (MD; Kadota and Shirasu, 2012). The main function of CTD's is to ensure the composition of homodimers and binding of cochaperones. The MD is important for recognition of the target protein, while NTD has an ATP binding site. (Cha *et al*. 2013).

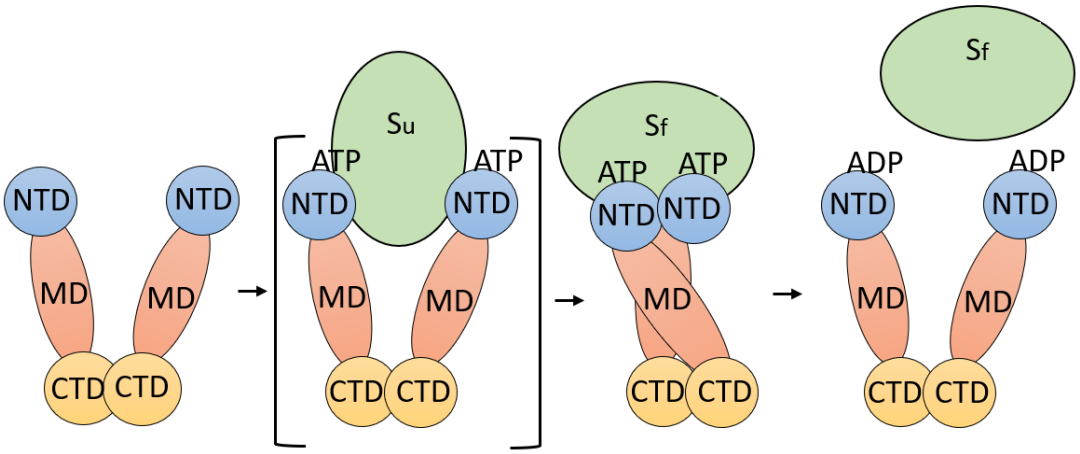

Figure 7: Structure and function of HSP90 dimer. The brackets include a short transition state. Abbreviations meaning: Su unfolded substrate; Sf folded substrate.

HSP90 can be found in the cell as monomer, dimer or in higher oligomeric states (Krishna *et al*., 1997). Dimer is considered to be a functionally active structure (Krishna and Gloor, 2001). Upon binding of ATP to NTD, the two monomers rotate, and NTDs connect to form a dimer or closed conformation, respectively. The dimer is now ATPase enzymatically active. Hydrolysis of the ATP molecule results in NTD rotation and separation, forming an open conformation of the dimer (Kadota and Shirasu, 2012). Transitions between the two dimer conformations ensure the chaperone role of HSP90 (Figure 7; Panaretou *et al*, 1998). HSP90 activity is regulated by posttranslational modifications (Franke *et al*., 2013) and cochaperones (Kadota and Shirasu, 2012).

2.4.2.5 Cytoplasmic heat shock proteins 90

Although this group is named cytoplasmic HSP90, cytoplasm is not the only place where they can be present, as they have been found in the nucleus.

The cytoplasmic HSP90s are highly homologous gene family as they share more than 96% of homology between them. All the genes for these proteins are located on the same chromosome in a 15 kb (Milioni and Hatzopoulos, 1997; Krishna and Gloor, 2001).

Cytoplasmic HSPs have a highly conserved CTD with a characteristic amino acid sequence of MEEVD called fingerprint (methionine, glutamic acid, glutamic acid, valine, aspartic acid, Johnson *et al*., 1998). For HSP90s, it is typical that chaperones

bind only non-native proteins (Pearl and Prodromou 2002). Furthermore, their chaperone function is substrate specific (Zhao *et al*., 2004).

There is increasing evidence about the involvement of HSP90s in the regulation of various developmental processes (Ludwig-Muller *et al*., 2000; Berardini *et al*., 2001; Ma *et al*., 2002). HSP90 as a chaperone affects the proper function of several other proteins including steroid hormone receptors, cell cycle kinases or proteins having a role in microtubule dynamics (Czar *et al*., 1997; Holt *et al.,* 1999; Pratt *et al*., 2001).

2.4.2.6 The function of HSP90.1 and HSP90.3

Important representatives of the HSP90 protein family in *A. thaliana* are HSP90.1 and HSP90.3. While the abundance of HSP90.1 protein in plants growing under normal conditions is relatively small, HSP90.3 level is higher in such conditions. For both proteins, increased abundance was observed under stress conditions (temperature stress, higher cadmium or arsenic content; Prasinos *et al.* 2004).

Changing environmental conditions can cause changes in the plant organism. In this context, HSPs work similarly to buffer solutions moderating the environmental influences that affect plant development (Sangster, 2004). HSP90.1 and HSP90.3 were studied in the context of embryonic development. HSP90.1 is expressed in very small amounts during early embryonic development, and the HSP90.1 protein level increases during seed maturation up to 30 times. HSP90.3 abundance follows a different trend as during early embryonic development, abundance is higher than HSP90.1, but during maturation, abundance increases only slightly (Prasinos *et al*., 2004).

Mutant plants *hsp90.1* and *hsp90.3* exhibit abnormal embryonic development. Furthermore, abnormalities are observed also in postembryonic development. The *hsp90.1* mutant phenotype exhibits abnormalities mainly in the root region. In the *hsp90.3* mutant, the unusual phenotype is manifested especially in cotyledons (Samakovli *et al*., 2007). This observation confirms that cytosolic HSP90s are involved in the proper development of embryonic pattern.

2.4.2.7 Gene expression of heat shock proteins under stress conditions

The expression of HSP genes is induced in several steps. First step involves activation of heat shock factors (HSF). Apart from heat stress (Mason *et al*., 1999; Xu et al.,

2010), HSF transcriptional factors are activated by other factors, such as drought (Rizhsky et al., 2002), or heavy metals (Courgeon et al., 1984).

Under normal conditions, HSFs are located in the cytoplasm as monomers and regulatory molecules, such as HSP70, bind HSF monomers to prevent HSF trimerization. Under stress conditions, the HSP70-HSF complex dissociates and, as a result, the formation of a trimer by three HSF monomers follows. (Larkindale *et al*., 2005). These trimers move to nucleus, where they bind the so-called heat shock element (HSE) HSE (Larkindale *et al*., 2005), DNA sequence found in gene promoters or regulatory sequences of HSP genes. HSE is highly conserved region with sequence 5‘-nGAAn-3‘ (5‘-n-glycine-alanine-alanine-n-3‘). After activation (interaction of HSF with HSE), the expression of HSP gene is triggered (Sorger and Nelson, 1989).

HSP gene expression is terminated by so-called negative feedback response. When there is excess of HSP over their target proteins, HSP70 binds to HSF leading to cessation of gene expression.

Despite their name, HSP proteins are induced not only by heat stress, but they are also expressed under normal conditions, though their overall abundance is lower (Rutherford and Lindquist, 1998; Mason *et al*., 1999).

3 Material and methods

3.1 Material

All chemicals used for the experiments are from Sigma Aldrich, Sigma Life Science, Duchefa Biochemistry and Life Technologies. Solutions and other material for molecular work were purchased from Thermo-Scientific, Sigma Aldrich and Nippon Genetics Europe GmbH.

3.1.1 Plant material

The primary plant material for mutant lines and control material was *Arabidopsis thaliana*, the Columbia ecotype (Col-0), or the Landsberg erecta (Ler) ecotype. All crossings were performed in the laboratories of the Department of Cell Biology of the Haná Region Center.

Experiments were conducted with the following mutant lines:

- *yda* - T-DNA insertion mutant, *yda1* (stop codon was inserted to the catalytic kinase domain; Lukowitz *et al.*, 2004)
- Δ*Nyda* – single mutant with the deletion of N-terminal regulatory sequence/domain of *yoda* gene; Lukowitz *et al*., 2004
- *mpk3-1* - T-DNA insertion mutant; SALK 151594
- *mpk6-2* - T-DNA insertion mutant; SALK 073907
- *hsp90.1* - T-DNA insertion mutant; SALK 007614
- *hsp90.3* - T-DNA insertion mutant; SALK 038646
- *pRac2::Hsp90RNAi* - RNAi line containing the antisense construct to HSP90 transcripts
- *hsp90.1yda* - T-DNA insertion double mutant
- *hsp90.3yda* - T-DNA insertion double mutant
- *hsp90.1*Δ*Nyda* - double mutant
- *hsp90.3*Δ*Nyda* - double mutant
- *pRac2::Hsp90RNAiyda* - double mutant
- *pRac2::Hsp90RNAi*Δ*Nyda* - double mutant
- WOX8::NLS:YFP – reporter line (WOX8 At5g45980); Ueda *et al*., 2011
- *yda* WOX8::NLS:YFP
- Δ*Nyda* WOX8::NLS:YFP

- *mpk3-1* WOX8::NLS:YFP
- *mpk6-2* WOX8::NLS:YFP
- *hsp90.1* WOX8::NLS:YFP
- *hsp90.3* WOX8::NLS:YFP

The plant material was planted on Petri dishes with ½ MS (Murashige and Skoog) medium. After the vernalization period (24h / 4 °C), the dishes were transferred to the phytotron. In the phytotron, the plant material was grown in a vertical position at photoperiodicity of 16h/light and 8h/dark at 25 °C. After two to four weeks, the plants were transplanted into the soil in circular pots. Plants in pots were grown in a phytotron at 16h/light and 8h/dark at 25 °C and were regularly watered.
Seeds for the next generation were harvested from eight- to ten-week old plants, which were allowed to dry at room temperature (25°C). The seeds were collected in paper bags attached to the plants.

3.1.2 Chemicals and laboratory devices

3.1.2.1 Commercially available solutions and chemicals

10x DreamTaq Buffer (Thermo-Scientific)
2-Mercaptoethanol (Sigma-Aldrich)
2x Phire Plant PCR Buffer (Thermo-Scientific)
37% hydrochlorid acid (Sigma-Aldrich)
4x Laemli Sample buffer (BioRad)
5x Phire Reaction Buffer (Thermo-Scientific)
6x DNA Loading Dye (6xLD; Thermo-Scientific)
Acrylamide/bis-acrylamide 37,5:1, 40% (BioRad)
Ammonium persulfate (APS, BioRad)
Agarose (Sigma Aldrich)
BSA (bovine serine albumin; Sigma-Aldrich)
Clarity TM Western ECL Substrate (BioRad): Luminol/enhancer solution and Peroxide/substrate solution
cOmplete, EDTA-free Protease Inhibitor Cocktail Tablets (Roche)
dNTP Mix (Thermo-Scientific)
DreamTaq DNA Polymerase (Thermo-Scientific)
Ethanol denat. 96% (Lihovar Kojetín)

GeneRuler™ 1 kb Plus DNA Ladder (Thermo-Scientific)

Incidur (Ecolab)

Isopropanol (Sigma-Aldrich)

Methanol (Sigma-Aldrich)

Midori Green Advance DNA stain (Nippon Genetics Europe GmbH)

N,N,N',N'-Tetramethylethylendiamin (TEMED, Sigma-Aldrich)

Phire Hot Start II DNA Polymerase (Thermo-Scientific)

PhosSTOP (Roche)

Ponceau S (Sigma-Aldrich)

RNase A (Thermo-Scientific)

Tween ® 20 (Sigma-Aldrich)

TGX Stain-Free™ FastCast™ Acrylamide Kit, 10% (BioRad)

3.1.2.2 Antibodies

Primary polyclonal rabbit anti-MPK3 (Sigma-Aldrich)

Primary polyclonal rabbit anti-MPK6 (Sigma-Aldrich)

Primary polyclonal rabbit anti-HSP90 (Santa Cruiz)

Primary polyclonal rabbit anti-pTEpY (anti-phospho-Threonine-Glutamic acid-phospho-Tyrosine; Biotech,)

Secondary goat anti-rabbit antibody labeled with horseradish peroxidase (Goat Anti-Rabbit IgG (HRP; Abcam)

3.1.2.3 Laboratory devices

Analytical balances (XA 110/2X, RADWAG, Waga Elektronicze)

Centrifuge Allegra (BeckmanCoulter)

Centrifuge ScanSpeed 1730 MR (LaboGene)

Deep freezer (Panasonic)

Electromagnetic stirrer IKA Combimag REO (Drehzahl Electronic)

Flowbox biohazard (Faster)

Gel imaging system ChemiDoc™ MP (BioRad)

ImageScanner™ III (GE Healthcare)

Laboratory fridge (Electrolux, Space Plus, ERB 34633W)

Laboratory hood (M1200, MERCI)

MyCycler™ Thermal Cycler (Bio-Rad)

NanoDrop (ThermoFisher)

pH meter (TEMP RS232, PL-600 pH/mV/Temp Meter, EZODO)

Phytotron (WEISS Gallenkamp)

Power supply BioRad Power Pac™Basic (BioRad)

Precision balances (S1502, BEL-Engineering)

Simplicity water purification system (Millipore)

T100™ Thermal Cycler (Bio-Rad)

Termoblok Thermocell Cooling&Heating Block CHB-202 (Bioer)

Viewer Gel Doc™ EZ Imager (Bio-Rad)

Vortex Genie -2 (Scientific Industries)

3.1.2.4 Microscopes

ApoTome microscope (Axio Imager M2, ZEISS)

Axio Zoom.V16 (ZEISS)

Confocal microscope (LSM 710, Axio Imager Z2, ZEISS)

Epifluorescence microscope (Axio Imager M2, ZEISS)

Stereo microscope (MSZ5000, A. Krüss)

3.1.2.5 Laboratory material

Eppendorf microtubes (1,5 ml; 2 ml), PVDC foils (Sarogold), beakers, volumetric cylinders, tweezers, Pasteur pipettes, filter paper, glass containers for membranes, cellulose wipes (KIMCHI), magnetic stirrers, sterile tips, scissors, sterile square Petri dishes

Appliances for acrylamide gel preparation (BioRad)

Appliances for agarose electrophoresis

Appliances for Western blotting (BioRad)

P 0.45 PVDF Blotting MembraneAmersham™ Hybond™ (GE Healthcare Life science)

3.1.2.6 Software

EPSON Scan software

ImageJ (Fiji 1.46r.)

Image Lab™ Software (Bio-Rad)

MS Office Excel 2016

ZEN Blue 2012 (ZEISS)

ZEN Black 2012 (ZEISS)

3.1.3 Solutions

Content of solutions prepared in the laboratory.

Sterilisation solution (50 ml):

- 5 ml 10% NaOCl (sodium hypochlorite; Sigma Aldrich)
- 45 ml ddH_2O (Sigma Life Science)
- 20 µl Tween 20 (Sigma Aldrich)

½ Murashige and Skoog (MS) $medium_{(s)}$ (1 l):

- 10 g sucrose (Sigma Aldrich)
- 8 g phytoagar (Sigma Aldrich)
- 2,15 g MS (Duchefa Biochemie)
- 1 g MES (2-(*N*-morpholino)ethanesulfonic acid; Sigma Aldrich)
- MilliQ H_2O added to 1l and adjust pH 5,8 with KOH

Edwards solution:

- 200 mM Tris-HCl pufr (pH 7,5; Sigma Aldrich)
- 250 mM NaCl (Sigma Aldrich)
- 25 mM EDTA (Sigma Aldrich)
- 0,5 % SDS (Sigma Aldrich)

TE buffer:

- 10 mM Tris-HCl (pH 8; Sigma Aldrich)
- 1 mM EDTA (Sigma Aldrich)

Extraction buffer for isolation of genomic DNA:

- 1% N-lauryl sarkosin (Sigma Aldrich)
- 100 mM Tris-HCl buffer (pH 8; Sigma Aldrich)
- 10 mM EDTA (pH 8; Sigma Aldrich)
- 100 mM NaCl (Sigma Aldrich)

1x TAE buffer:

- 40 mM Tris-HCl (Sigma Aldrich)
- 20 mM acetic acid (Sigma Aldrich)
- 1 mM EDTA (pH 8; Sigma Aldrich)

Fixative solution:

- 50 % methanol (Sigma Aldrich)
- 10 % acetic acid (Sigma Aldrich)

Periodic acid (1%):

- 0,1 mg solid periodic acid (Sigma Aldrich)
- 10 ml dH_2O

Schiff reagent with propidium iodide:

- 260 µl sodium bisulphite 40% ≈ 3,8 M (Sigma Aldrich)
- 190 µg sodium metabisulphite (Sigma Aldrich)
- 125µl HCl 37% (Sigma Aldrich)
- 1 µg propidium iodide (Life Technologies)
- First pour 5 ml of water into a 10 ml container, then add HCl, sodium bisulphite or sodium metabisulphite, and propidium iodide. Finally add water to 10 ml.

Extraction buffer for protein isolation (EB_p, 200ml):

- 0,7268 g 30 mM Tris base
- 2 ml glycerol
- 1,752 g 150 mM NaCl
- 4 ml 0,5 M EDTA
- 200 µl 1M NaF
- 1mM DTT add before using EB_p
- cOmplete, PhosSTOP 1 tablete for 10 ml of buffer, add before using EB_p

Transfer buffer 10x (TB):

- 30g Tris(hydroxymethyl)aminomethan (Sigma-Aldrich)
- 144g Glycine (Sigma-Aldrich)
- MilliQ H_2O added to 1l

Transfer buffer 1x (TB):

- 100 ml TB 10x
- 100 ml methanol (100%, Sigma Aldrich)
- 800 ml MilliQ H_2O

Tris buffered saline 10x (TBS):

- 24 g Tris(hydroxymethyl)aminomethan (Sigma-Aldrich)

- 87,8 g NaCl (Sigma Aldrich)
- MilliQ H_2O added to 1l and adjust pH to 7,4 with HCl

TBS-T buffer:

- 100 ml TBS 10x
- 900 ml MilliQ H_2O
- 1 ml Tween 20 (Sigma Aldrich)

Running buffer 10x (RB):

- 30 g Tris(hydroxymethyl)aminomethan (Sigma-Aldrich)
- 144 g Glycine (Sigma Aldrich)
- 10 g sodium dodecylsulphate (SDS, Sigma Aldrich)
- MilliQ H_2O added to 1l

Running buffer 1x (RB):

- 100 ml RB 10x
- 900 ml MilliQ H_2O

Resolving gel (10% acrylamide):

- 3,0313 ml dd H_2O
- 1,5625 ml Acrylamide/bis-acrylamide 37,5:1, 40% (BioRad)
- 1,5625 ml 1,5 M Tris buffer (pH 8,8)
- 62,5 µl 10% SDS
- 31,25 µl 10% APS (BioRad)
- 3,125 µl TEMED (Sigma-Aldrich)

Stacking gel (4% acrylamide)

- 795 µl dd H_2O
- 125 µl Acrylamide/bis-acrylamide 37,5:1, 40% (BioRad)
- 315 µl 0,5 M Tris buffer (pH 6,8)
- 12,5 µl 10% SDS
- 6,25 µl 10% APS (BioRad)
- 1,25 µl TEMED (Sigma Aldrich)

Stain free resolving gel (TGX Stain-Free™ FastCast™ Acrylamide Kit, 10%; BioRad):

- 3 ml Resolving gel solution A
- 3 ml Resolving gel solution B
- 30 µl 10% APS (BioRad)
- 3 µl TEMED (Sigma Aldrich)

Stain free stacking gel (TGX Stain-Free™ FastCast™ Acrylamide Kit, 10%; BioRad)

- 1 ml Stacking gel solution A
- 1 ml Stacking gel solution B
- 10 µl 10% APS (BioRad)
- 2 µl TEMED (Sigma Aldrich)

3.2 Methods

3.2.1 Seed sterilization

Chemicals:

- Sterilization solution (50 ml)

Workflow:

1. Small amount of seeds was transfered into 1,5 ml Eppendorf.
2. 1 ml of sterilization solution (1% sodium hypochlorite) was added and vortexed.
3. After 20 minutes, the sterilization solution was removed, and the seeds were washed for 1 minute in 1 ml of 70% ethanol.
4. After removing ethanol, the seeds were washed four times with distilled deionized water.
5. This way sterilized seeds can be planted on a Petri dish or stored in water at 4 °C.
6. The Petri dishes with planted seeds were placed for 24 hours at a temperature of 4 °C, thus the seeds pass through the vernalization stage. Then were the Petri dishes transferred to the phytotron.

3.2.2 Preparation of ½ MS solid medium

Chemicals:

- ½ MS medium (1 l)

Workflow:

1. 200 ml of water was poured into a 1-liter beaker and sucrose, MS and MES were added.
2. The pH was adjusted to 5,75 with KOH and MilliQ H_2O was added to 1 l.
3. Within four 500 ml bottles, 2 g of phytoagar were weighted and to each flask was poured 250 ml of solution. The medium was sterilized in autoclave (30 minutes at 121 °C and high pressure).

3.2.3 Genotyping

3.2.3.1 DNA extraction using commercially available kit

The MagMAX plant DNA isolation kit (Thermo Scientific) was used.

Chemicals:

- Dilution solution

Workflow:

1. 20 µl of delution solution was pipetted to the 1,5 ml Eppendorf.
2. Leaf was cut by sterile scissors under aseptic condition and transferred into the dilution solution. Using a tip, the leaf was resuspended in the dilution solution and the Eppendorf was placed on ice.
3. The homogenate was stored on ice for at least 20 minutes or to the next day at – 20 °C.

3.2.3.2 DNA isolation using Edward's solution

Chemicals:

- Edward‘s solution
- TE buffer

Workflow:

1. The extraction buffer was prepared by diluting the Edwards solution with TE buffer in a ratio of 1: 9.
2. 80 µl of extraction buffer was pipetted into the prepared 1,5 ml Eppendorf.

3. Leaf was cut with sterile scissors in aseptic conditions and transfered to the extraction buffer. Using a tip, the leaf was resuspended in the dilution solution and the Eppendorf was placed on ice.
4. The homogenate was stored for at least 20 minutes on ice or to the next day at – 20 °C.

3.2.3.3 Genomic DNA isolation

Material:

- 1,5 ml Eppendorf pre-frozen in liquid nitrogen
- pre-frozen crusher
- pre-cooled stand
- pre-cooled centrifuge (4 °C)
- digester

Chemicals:

- extraction buffer
- phenol-chloroform-isoamyl alcohol solution in ratio 25:24:1
- 3 M sodium acetate (CH_3COONa; pH 5,2)
- pre-frozen ethanol
- 70% ethanol
- TE buffer (pH 8) with RNAsa A (1 µl /1 ml TE pufru)

Workflow:

1. About 5 to 10 young leaves (200-400 mg) were collected into pre-frozen 1,5 ml Eppendorf.
2. Leaves were crushed into a fine powder, while cooling the test tubes in liquid nitrogen.
3. 800 µl extraction buffer was added to the frozen test tube with leaves powder. The mixture was vortexed for 30 sec.
4. 800 µl of phenol-chloroform-isoamyl alcohol solution was added to the mixture and vortexed again for 30 seconds.
5. After sufficient mixing, the samples were centrifuged in a pre-cooled centrifuge (4 °C) at 5000 rpm for 3 minutes.
6. The supernatant was divided into two phases by centrifugation. The lower (aqueous) phase in which the genomic DNA was dissolved was carefully

pipetted into another 1,5 ml Eppendorf so that the interface between the phases was not broken.

7. 80 ml of 3 M CH_3COONa was added to the solution and 800 µl of pre-frozen ethanol was added to the mixture, to precipitate DNA.
8. Samples were centrifuged at 13,000 rpm for 10 minutes in a pre-cooled centrifuge (4 °C).
9. Supernatant was carefully removed from the samples. The precipitate was washed with 800 µl of 70% ethanol.
10. Samples were centrifuged at 13,000 rpm for 5 minutes in a pre-cooled centrifuge (4 °C).
11. The supernatant was removed, and the precipitate was left to dry at room temperature (25 °C) for 30 minutes.
12. To the precipitate was added 100 µl of TE buffer (pH 8) with added RNase A and the solution was incubated for 1 h at 37 °C.
13. The final genomic DNA solution is stored at -20 °C.

3.2.3.4 PCR with the Phire II enzyme

Chemicals:

- Master Mix for 1 sample using 2x Phire Plant PCR Buffer
    - 10 µl 2x Phire Plant PCR Buffer
    - 6,6 µl ddH_2O
    - 1 µl primer forward
    - 1 µl primer reverse
    - 0,4 µl Phire Hot Start II DNA Polymerase (Thermo-Scientific)
- Master Mix for 1 sample using 5x Phire Reaction Buffer
    - 4 µl 5x Phire Reaction Buffer
    - 12,2 µl ddH_2O
    - 0,4 µl 10 nM dNTPs
    - 1 µl primer forward
    - 1 µl primer reverse
    - 0,4 µl Phire Hot Start II DNA Polymerase (Thermo-Scientific)

Workflow:

1. To prepare Master Mix, the desired quantity of individual solutions was pipetted into the 1,5 ml Eppendorf according to the number of samples.
2. Master Mix was vortexed before use to mix the individual components of the solution. After the enzyme was added it is necessary to work on ice.
3. 19 µl Master Mix was pipetted to the microtiter plate or individual strips. Then was added 1 µl of the solution with the isolated DNA.
4. Microtiter plate or strips were closed, and the samples were vortexed.
5. According to Table 1, the Thermal Cycler was set. Annealing temperature (Ta respectively TaPhire) corresponds to temperatures in Table 2.

Table 1. Thermal Cycler (T100™ Thermal Cycler Bio-Rad; MyCycler™ Thermal Cycler Bio-Rad) setting for PCR reaction with Phire Hot Start II DNA Polymerase

process	temperature	time	number of repetition
iniciation	98 °C	3 min	1x
denaturation	98 °C	5 s	
annealing	TaPhire	5 s	40x
extension	72 °C	40 s	
final extension	72 °C	5 min	1x
hold	4 °C	∞	

Table 2 Sequences of primers used for PCR and annealing temperature of Phire Hot Start II DNA Polymerase and DreamTaq DNA Polymerase. Ta was calculated by program at Thermo-Scientific website (https://www.thermofisher.com/cz/en/home/brands/thermo-scientific/molecular-biology/molecular-biology-learning-center/molecular-biology-resource-library/thermo-scientific-web-tools/tm-calculator.html 25.3.2019)

gene	primer	sequence	TaPhire	TaDreamTaq
mpk3-1	forward	5'-ATT TTT GTC AAC AAT GGC CTG-3'	61,0	49,1
	reverse	5'-TCT GCC TTT TCA CGG AAT ATG-3'		
mpk6-2	forward	5'- CTCTGGCTCATCGCTTATGT -3'	62,7	50,1
	reverse	5'- ATCTATGTTGGCGTTTGCAAC -3'		
LBb1.3	forward	5'-ATT TTG CCG ATT TCG GAA C-3'		
HSP 90.1	forward	5'-TCA GAC CCA ACT TCA ACA TCC-3'	62,7	50,8
	reverse	5'-TGA CCA ATG ACT GGG AAG ATC-3'		
HSP 90.3	forward	5'-TCC ATA GGT TAT TGC ACT GGC-3'	61,9	49,5
	reverse	5'-CAC AAA AAG CTT CGC AAC TTC-3'		
LBb1	forward	5'-GCG TGG ACC GCT TGC TGC AAC T-3'		

3.2.3.5 Dream Taq PCR

Chemicals:

- Master Mix for 1 sample using DreamTaq DNA Polymerase (Thermo-Scientific)
    - 5 µl 10x DreamTaq Buffer (Thermo-Scientific)
    - 5 µl 2mM dNTPs (Thermo-Scientific)
    - 1 µl primer forward
    - 1 µl primer reverse
    - 0,25 µl DreamTaq DNA Polymerase (Thermo-Scientific)
    - 37,75 µl ddH_2O

Workflow:

1. To prepare Master Mix, the desired quantity of individual solutions was pipetted into the 1,5 ml Eppendorf according to the number of samples.
2. Master Mix was vortexed before use to mix the individual components of the solution. After the enzyme was added it is necessary to work on ice.
3. 19 µl Master Mix was pipetted to the microtiter plate or individual strips. Then was added 1 µl of the solution with the isolated DNA.
4. Microtiter plate or strips were closed, and samples were vortexed.
5. According to Table 3, the Thermal Cycler was set. Annealing temperature (Ta respectively TaDreamTaq) corresponds to temperatures in Table 2.

Table 3 Thermal Cycler (T100™ Thermal Cycler Bio-Rad; MyCycler™ Thermal Cycler Bio-Rad) setting for PCR reaction with DreamTaq DNA Polymerase enzyme

process	temperature	time	number of repetition
iniciation	95°C	3 min	1x
denaturation	95°C	30 s	
annealing	TaDreamTaq	30 s	40x
extension	72°C	40 s	
final extension	72°C	5 min	1x
hold	4°C	∞	

3.2.3.6 DNA electrophoresis

Material:

- Electrophoretic equipment (Bio-Rad) and voltage source (Bio-Rad)
- Viewer Gel Doc™ EZ Imager (Bio-Rad) and PC software Image Lab™ Software (Bio-Rad)

Chemicals:

- agarose (Sigma Aldrich)
- 1x TAE buffer
- Midori Green Advance DNA stain (Nippon Genetics Europe GmbH)
- GeneRuler^{TM} 1 kb Plus DNA Ladder (Sigma-Aldrich)
- 6x DNA Loading Dye (6xLD; Thermo-Scientific)

Workflow:

1. The exact amount of agarose was weighed so that the resulting solution concentration was 1 %. Agarose was transferred to the Erlenmeyer flask and required amount of 1x TAE buffer was added.
2. The mixture was warmed in a microwave oven, until agarose dissolved.
3. When agarose mixture cooled down, but still did not start to solidify, Midori Green Advance DNA stain was added. Than the solution was mixed.
4. The mixture was poured into the prepared sealed bathtub for the electrophoretic gel. The resulting bubbles were removed. A comb was placed in the bathtub and the gel was left to solidify at room temperature for 20 minutes.
5. After solidification, the gel was transferred to an electrophoretic bath filled with 1x TAE buffer.
6. 6x DNA Loading Dye was added to the PCR reaction samples to be six times diluted.
7. 5 µl of GeneRuler ™ 1 kb Plus DNA Ladder was loaded to the first well in the gel. 10 µl of samples with LD were pipetted to the other wells.
8. Electrophoretic separation was taking place at a constant electrical voltage of 5 V/cm for 30 minutes.
9. The gel was then scanned using the Gel DocTM EZ Imager (Bio-Rad) and evaluated using Image LabTM Software (Bio-Rad).

3.2.4 Protein analysis

3.2.4.1 Tissue homogenization and protein extraction

Material:

- Wild type plant Col-0 and *hsp90.1, hsp90.3, pRac2::hsp90RNAi, mpk3-1* and *mpk6-2* single mutants
- Pre-frozen mortar and pestle

Chemicals:

- Liquid nitrogen (N_L)
- Extraction buffer

Workflow:

1. First siliques were harvested and put into a mortar with liquid nitrogen. Tissue was homogenized with pestle, while cooling the equipment in liquid nitrogen. The fine powder was transferred to a pre-frozen Eppendorf and frozen in liquid nitrogen.
2. Samples can be stored in deep freezer (-80 °C).
3. Extraction buffer was pipetted into the Eppendorf with sample to have volume ratio 1:1 and microtube was gently mix by agitation. Mixture was incubated for 30 to 60 minutes (depending on the amount of the sample) on ice.
4. Microtubes were centrifuged 30 minutes at 13 000 rpm in 4 °C. Liquid phase (supernatant) was pipetted to new microtube and centrifugated 5 minutes at 15 000 rpm in 4 °C. Liquid phase was transferred to clean microtube.
5. Protein concentration in sample was measured using NanoDrop. An extraction buffer was used as a reference sample (blank). The samples were diluted to the desired protein concentration.
6. To the sample was added 4x Laemli Sample buffer with 5 % mercaptoethanol, to volume ratio 3:1 of sample to 4x Laemli with mercaptoethanol. Proteins ware denaturated at 95 °C for 10 minutes.
7. Samples can be stored in deep freezer (-80 °C).

3.2.4.2 Preparation of classical acrylamide gels for electrophoresis

Material:

- Stacking and resolving gels
- Equipment for gel preparation (BioRad)

Workflow:

1. Equipment for gel preparation was properly washed and cleaned with 100% methanol. Apparatus for the preparation of acrylamide gel was prepared to be tightly sealed.
2. The individual resolving gel components were mixed and the mixture was pipetted between the glasses. The gel was covered with a small amount of

isopropanol and left to polymerize for 30 minutes at room temperature. Than isopropanol was removed.

3. The individual stacking gel components were mixed, and the mixture was pipetted on resolving gel between the glasses. The comb was immersed in the stacking gel, which polymerized at room temperature for 20 minutes.

3.2.4.3 Preparation of stainfree acrylamide gels for electrophoresis

Material:

- TGX Stain-Free™ FastCast™ Acrylamide Kit, 10% (BioRad)
- Equipment for gel preparation (BioRad)

Workflow:

1. Equipment for gel preparation was properly washed and cleaned with 100% methanol. Apparatus for the preparation of acrylamide gel was prepared to be tightly sealed.
2. The individual resolving gel components were mixed and the mixture was pipetted between the glasses. The individual stacking gel components were mixed, and the mixture was pipetted on resolving gel between the glasses. The comb was immersed in the stacking gel, which polymerized at room temperature for 20 minutes.

3.2.4.4 Protein electrophoresis

Material:

- Equipment for electrophoresis (BioRad)
- Power supply BioRad Power Pac^{TM}Basic (BioRad)
- Running buffer (1x)

Workflow:

1. Acrylamide gels between glasses were put into plastic holder into electrophoresis bathtub. Running buffer was poured into the bathtub. The comb was removed, and samples and marker were pipetted into the wells.
2. A 24V power supply (BioRad Power Pac^{TM}Basic (BioRad) was connected. The procedure of electrophoresis itself was 1,5 hour long.

3.2.4.5 Protein visualization in gel

After electrophoresis Stain-free gels were visualized by gel imaging system ChemiDoc^{TM} MP (BioRad).

3.2.4.6 Protein transfer to membrane

Material:

- Equipment for protein transfer from gel to membrane (BioRad)
- Transfer buffer (1x)
- Power supply BioRad Power Pac^{TM}Basic (BioRad)

Workflow:

1. All necessary tools for transfer were prepared and incubated in transfer buffer. The membrane was incubated one minute in 100% methanol. Stacking gel was removed from resolving gel.
2. A pad, two filter papers, the resolving gel, the transfer membrane, two filter papers and a sponge were placed between the support grid. The sandwich was fixed to the transfer tank, which was filled with transfer buffer. A cooler was placed in the bathtub.
3. Transfer tank was connected to power supply. Transfer was processed from cathode to anode with support of 24 V power over night at 4 °C.

3.2.4.7 Membrane visualization

To see if the transfer from non-stain-free gels was successful and for loading control, it is necessary to visualize the proteins on the membrane.

Workflow:

1. Membranes were stained with 0,2 M Ponceau for 5 minutes. Subsequently, Ponceau was washed out with MilliQ H_2O two times for 10 minutes at 50 rpm, membrane was dried and photographed. Staining was removed by washing membrane for 30 seconds in methanol, then was membrane washed three times 10 minutes in TBS-T.

3.2.4.8 Western blot analysis using specific antibodies

Material:

- BSA, Clarity^{TM}Western ECL Substrate (Bio-Rad), TBS-T

Table 5 List of primary and secondary antibodies and their dilution in TBS-T

antibody	dilution in TBS-T
primary polyclonal rabbit anti-pTEpY	1:1000
primary polyclonal rabbit anti-MPK3	1:3000
primary polyclonal rabbit anti-MPK6	1:16000
primary polyclonal rabbit anti-HSP90	1:1000
secondary Goat Anti-Rabbit IgG (HRP)	1:5000

Workflow:

1. Membrane was blocked to improve specific binding of primary antibody by incubating with 5% BSA solubilized in TBS-T over night at 4 °C and under shaking (10 rpm).
2. After blocking agent was removed membrane was incubated with primary antibody (listed in Table 5) in 5% BSA in TBS-T over night at 4 °C and under shaking (10 rpm).
3. Unbound or non-specifically bound primary antibody residues were washed from the membrane with TBS-T six times for 10 minutes at room temperature at 50 rpm.
4. The membrane was incubated with a secondary antibody (Table 5) in 1% BSA in TBS-T for two hours at room temperature and 10 rpm.
5. Unbound or non-specifically bound secondary antibody residues were washed from the membrane with TBS-T three times for 10 minutes at room temperature at 50 rpm.
6. To visualize specific protein the Clarity^{TM}Western ECL Substrate (Bio-Rad) kit was used. Solution of luminol and peroxide was mixed according to the instructions and the membrane was incubated for 60 seconds in the resulting mixture. Then the membrane was inserted into the gel imaging system ChemiDoc^{TM} MP (BioRad). ImageLab software was used to take images of the membrane. Firstly, colorimetric scanning was made to visualize the marker. The secondary antibody was labeled with horseradish peroxidase that catalyzed the oxidation of luminol in presence of peroxide, meaning that this reaction generated light. Thus, with the high sensitivity function for luminescence, the proteins were visualized.

3.2.4.9 Membrane stripping for removal of antibodies

Workflow:

1. Protein-bound membrane can be used to visualize multiple specific proteins. It is necessary to remove bound antibodies from the membrane for this procedure. Thus, the membrane was washed in 0,5 M NaOH solution two times for 20 minutes at laboratory temperature and 50 rpm.
2. Membrane was washed 10 minutes in ddH_2O and three times for 10 minutes in TBS-T.

3. After this treatment steps, the process described in chapter 2.2.4.8. "Visualization of proteins using specific antibodies" can be performed again with the same membrane.

3.2.5 Phenotyping

3.2.5.1 Primary root development

Workflow:

1. Seeds of wild-type plants the Col-0 and Ler ecotypes and single Δ*Nyda*, *yda*, *mpk3-1*, *mpk6-2*, *hsp90.1*, *hsp90.3*, *pRac2::Hsp90RNAi* mutants and *hsp90.1yda*, *hsp90.3yda*/+, *hsp90.1*Δ*Nyda*, *hsp90.3*Δ*Nyda* double mutants were planted on Petri dishes with ½ MS solid media. All mutants were represented by at least 30 samples.
2. After the vernalization period (24 h / 4° C), the dishes were transferred to the phytotron. In the phytotron, the plant material was grown in a vertical position at photoperiodicity of 16 h/light and 8 h/dark at 25 °C for seven days.
3. After five and seven days respectively, growing seedlings were scanned.
4. Length of roots was measured in ImageJ (Fiji 1.46r.) software, length was recalculated from pixels to millimeters with the enclosed ruler.
5. To statistically verify observation One-way ANOVA (ANALYSIS OF VARIANCE) with post-hoc Tukey HSD (Honestly Significant Difference) tests were used (http://astatsa.com/OneWay_Anova_with_TukeyHSD 2.3.2019).

3.2.5.2 Reproductive phase – floral development

Material:

- One month old plants of wild-type the Col-0 and Ler ecotypes and single Δ*Nyda*, *yda*, *mpk3-1*, *mpk6-2*, *hsp90.1*, *hsp90.3*, *pRac2::Hsp90RNAi* mutants and *hsp90.1yda*, *hsp90.3yda*/+, *hsp90.1*Δ*Nyda*, *hsp90.3*Δ*Nyda* double mutants in pots.

Workflow:

1. The inflorescence was cut about a centimeter and a half from the top of the flower meristem and was stuck in ½ MS solid media in a Petri dish.
2. For all mutants, three samples were prepared and each was imaged from above and from the side using AxioZoom V.16 microscope. The objective

magnification was 8x. A center lamp on the lens with intensity 25% was used for illumination, the exposure time was 27,000 ms. Measurement and adjusting the brightness and contrast of images was done using the ZEN blue edition 2012 software.

3.2.5.3 Epifluorescence microscopy observation

Material:

- WOX8::NLS:YFP – reporter line (WOX8 At5g45980), from Ueda *et al*., 2011
- *yda*WOX8::NLS:YFP, Δ*Nyda*WOX8::NLS:YFP, *mpk3-1*WOX8::NLS:YFP, *mpk6-2*WOX8::NLS:YFP, *hsp90.1*WOX8::NLS:YFP and *hsp90.3*WOX8::NLS:YFP.

Workflow:

1. Five siliques from flower meristem were harvested from plants and put onto the microscope slide into drop of water. These siliques were gently slit opened in replum.
2. Embryos were removed from siliques using tweezer and needle. Samples were covered with cover glass.
3. Samples were observed on epifluorescence microscope using three channels. To determine the developmental stage of embryo channel for DIC (differential interference contrast) was used with light source intensity 2.33 V. To observe signal from YFP protein channel AF488 was used with filter excitation 450 – 490 nm and filter emission 545 – 565 nm. In addition, channel DsRed was used to to verify that the observed signal is not autofluorescence or other nonspecificity with . For imaging, magnification 20x or 40x was used.

3.2.5.4 Modified pseudo-Schiff propidium iodide staining

The protocol for modified pseudo-Schiff propidium iodide (mPS-PI) staining of ovules and seeds was performed as previously described (Truernit, *et al.*, 2008).

Chemicals:

- Fixative solution
- Periodic acid 1%
- Schiff reagent with propidium iodide

Workflow:

Day 1:

1. Siliques from flower meristem were harvested from plants and gently incised on one side.
2. The siliques were put in fixative solution and incubated at 4 °C for at least 12 hours (up to 1 month).

Day 2:

3. The siliques were rinsed with water two times and treated with 1% SDS and 0.2 M NaOH. Samples were incubated at room temperature over night.

Day 3:

4. The siliques were rinsed with water three times.
5. Next step was treatment with 10% bleach solution (sodium hypochlorite) for 5 minutes (until siliques were colourless).
6. Then, siliques were rinsed with water three times.
7. The siliques were treated with 1% periodic acid at room temperature for 40 minutes.
8. The siliques were rinsed with water three times.
9. The siliques were treated with Schiff reagent with propidium iodide for 2 hours until siliques were stained (dark pink).
10. The propidium iodide solution was exchanged for a solution of chloral hydrate, and as such were stored. Alternatively, siliques were transferred directly onto a microscope slide. Embryos were removed from siliques using tweezer and needle and samples were mounted in chloral hydrate. After covering with cover glass, the edges were coated with nail polish.
11. The samples were left to stabilize for free days in room temperature and then were observed with CLSM microscope. To visualize embryos, 40x objective (Plan Apochromat, N_A = 1.4, work distance with cover glass 0,17 mm, ZEISS) with immersion oil. For imaging, laser with wavelength 514 nm and with intensity 2 %, the filter for 566 – 719 nm and beam splitter 458/514 were employed. The pinhole was set for 90 µm and the pixel dwell was 6.3 µs.

4 Results and discussion

In the present thesis we focused on the interaction of YODA-MAPK cascade and HSP90. Previously published results show that HSP90 interacts with YODA and modulates the downstream MAPK signalling cascade to control stomata development. Moreover, YODA-MAPK cascade is known to affect asymmetric divisions which are important in the development of the embryo and primary root (Lukowitz *et al.,* 2004; Smékalová *et al*., 2014). To further investigate the impact of HSP90 and YODA genetic interaction on plant development, we decided to study both the effects of HSP90/YODA genetic interactions during the vegetative and reproductive phase of plant development. For this reason, we performed phenotypic analysis of primary root development, development of flowers, and early embryonic development in single *hsp90* and YODA cascade mutants and double *hsp90yda* mutants.

4.1 Phenotype characterisation

4.1.1 Root length of single and double mutants

To analyse root development, we used 5 and 7 dpg (days post germination) seedlings of wild-type plants the Col-0 and Ler ecotypes and single and double mutant plants such as Δ*Nyda*, *yda, mpk3-1, mpk6-2, hsp90.1*, *hsp90.3*, *pRac2::Hsp90RNAi* for single mutants and *hsp90.1yda*, *hsp90.3yda*/+, *hsp90.1*Δ*Nyda*, *hsp90.3*Δ*Nyda* for double mutants. All of the mentioned mutants are homozygous except for *hsp90.3yda*/+, where homozygots are embryo-lethal. *Yda*, Δ*Nyda* and *hsp90.3*Δ*Nyda* mutants are unable to produce fertile seeds, so genotypic characterization is required to confirm the genotype in each generation.

Seedlings growing in Petri dishes were scanned and pictures were processed by ImageJ (Fiji 1.46r.) software. Each of the mutant lines was represented by thirty seedlings. The data were processed using MS Excel 2016 whereby all the charts were created. We used One-way ANOVA (ANALYSIS OF VARIANCE) with post-hoc Tukey HSD (Honestly Significant Difference) tests for statistical analysis in order to evaluate significant differences in primary root length among the studied mutants (ASTATSA: http://astatsa.com/OneWay_Anova_with_TukeyHSD/ 25.11. 2018).

First, the single mutants in the *YDA* gene (*yda* and *ΔNyda*) showed a significant difference in the root length (compared to the Ler ecotype; Figure 8A and B). Roots of *yda* mutant seedlings were significantly shorter and atypically growing lateral roots

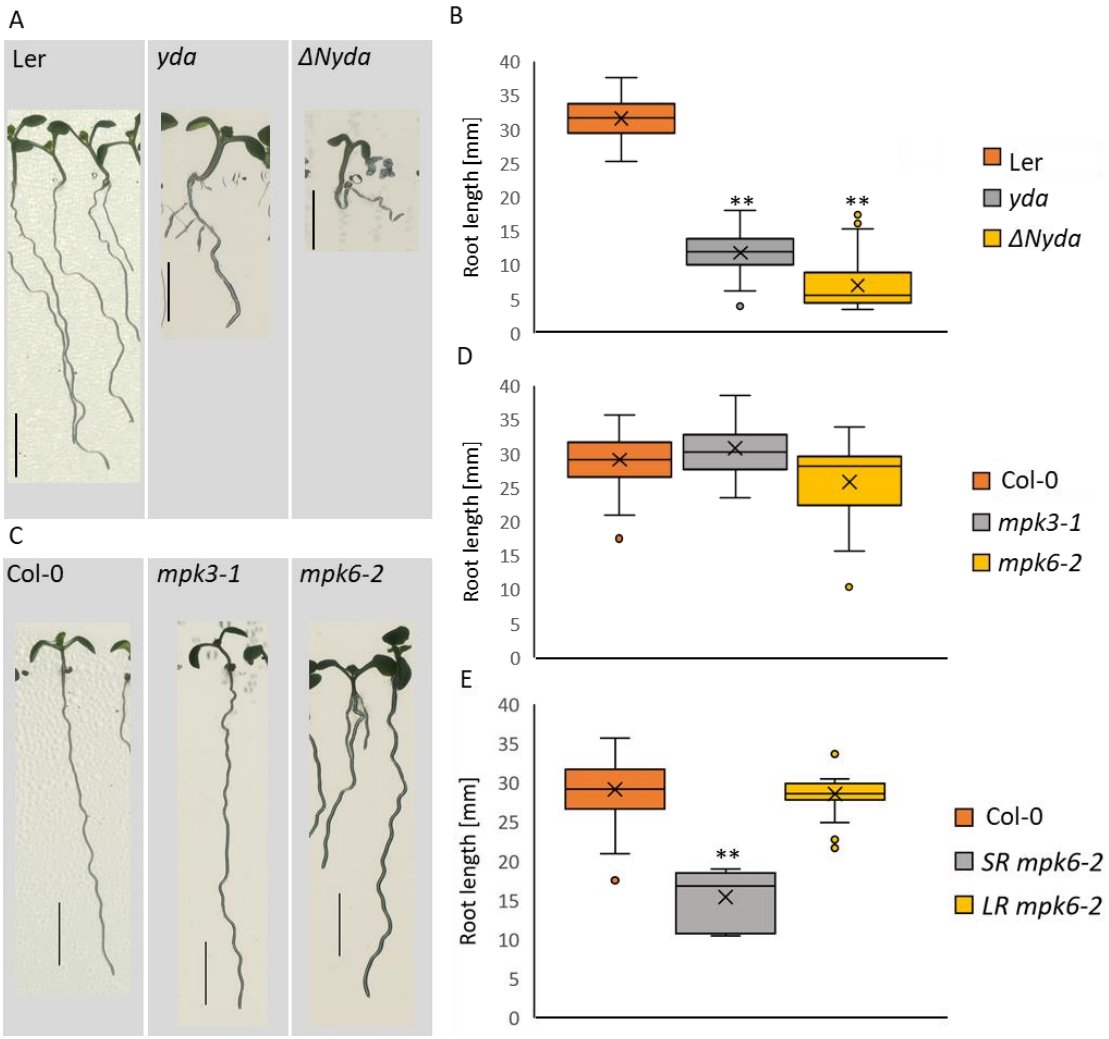

Figure 8: Primary root development in WT and YODA-MAPK cascade mutants. *yda* and *ΔNyda* roots phenotypical observation (A) and statistical analysis of root length (B). *mpk3-1* and *mpk6-2* mutant phenotypes (C) and statistical analysis of root length (D). Additional graph (E) is showing differences in two *mpk6-2* root phenotypes. All measurements show 5 mm. Double asterisk means significant difference from wild-type by p value ($p < 0.01$; Tukey test).

occurrence was observed (Figure 8A *yda*). The roots of the *ΔNyda* mutant were also significantly shorter and twisted (Figure 8A *ΔNyda*).

Next, we studied the root length of mutants *mpk3-1* and *mpk6-2*, as mutants deficient for MAPK, which are part of the YODA-MAPK signaling cascade. The phenotype of *mpk3-1* primary roots did not differ significantly from the control.

It has been previously reported that the primary root of the *mpk6-2* mutant is found in three phenotypic variants – no-root (10 %), short-root (20 %) and long-root (70 %) (Lopéz-Bucio *et al.*, 2014). Due to the small number of seedlings we used, we were not able to significantly differentiate the *mpk6-2* mutant line from wild-type, however,

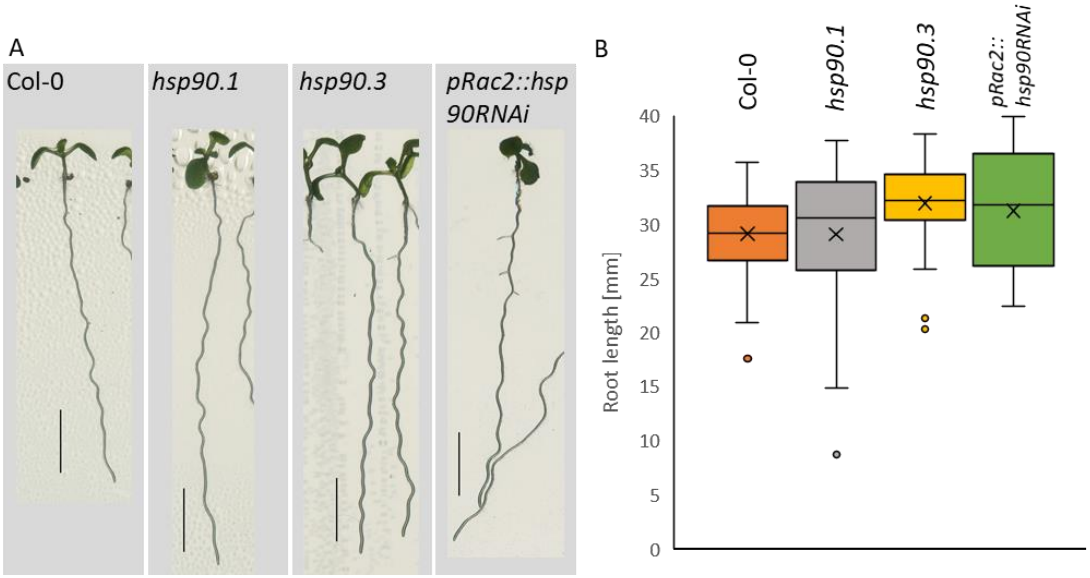

Figure 9: Primary root development in WT and HSP90 mutants. Phenotypical (A) and statistical (B) analysis of root development. All measurements show 5 mm. Any mutant was significantly different from wild-type by p value *(*$p < 0.01$*;* Tukey test).

from the phenotypic analysis the difference was noticeable (Figure 8E and F). Because of the low frequency of no-root phenotypic variant, this trend did not appear in our statistical set. Unlike the no-root phenotype, we observed the occurrence of the short root and long root phenotypes. For additional information, we added a box plot graph comparing only wild-type with phenotypic variants of *mpk6-2* primary root (Figure 8E).

Furthermore, we analysed *hsp90* mutants (Figure 9). Although we visually assessed that the *hsp90* roots were slightly longer than the control sample (Figure 9A), it was not a statistically significant difference (Figure 9B).

Analysis of the primary root length in *hsp90.1yda* and *hsp90.3yda/+* double mutants showed no significant differences compared to *hsp90* single mutants nor to the wild-type plants (Figure 10A, B), suggesting that *hsp90* genetic depletion can rescue the severe phenotype of *yda* mutant.

Interestingly, the analysis of primary root length in *hsp90ΔNyda* mutants showed greater phenotypic variation (Figure 10A, C). This phenotypic variation was depicted by the broader range of the root length phenotypes of *hsp90.1ΔNyda* plants, which

ranged from short root to long root plants. This is easily visible by the wide range between first and fourth quartiles in Figure 10B.

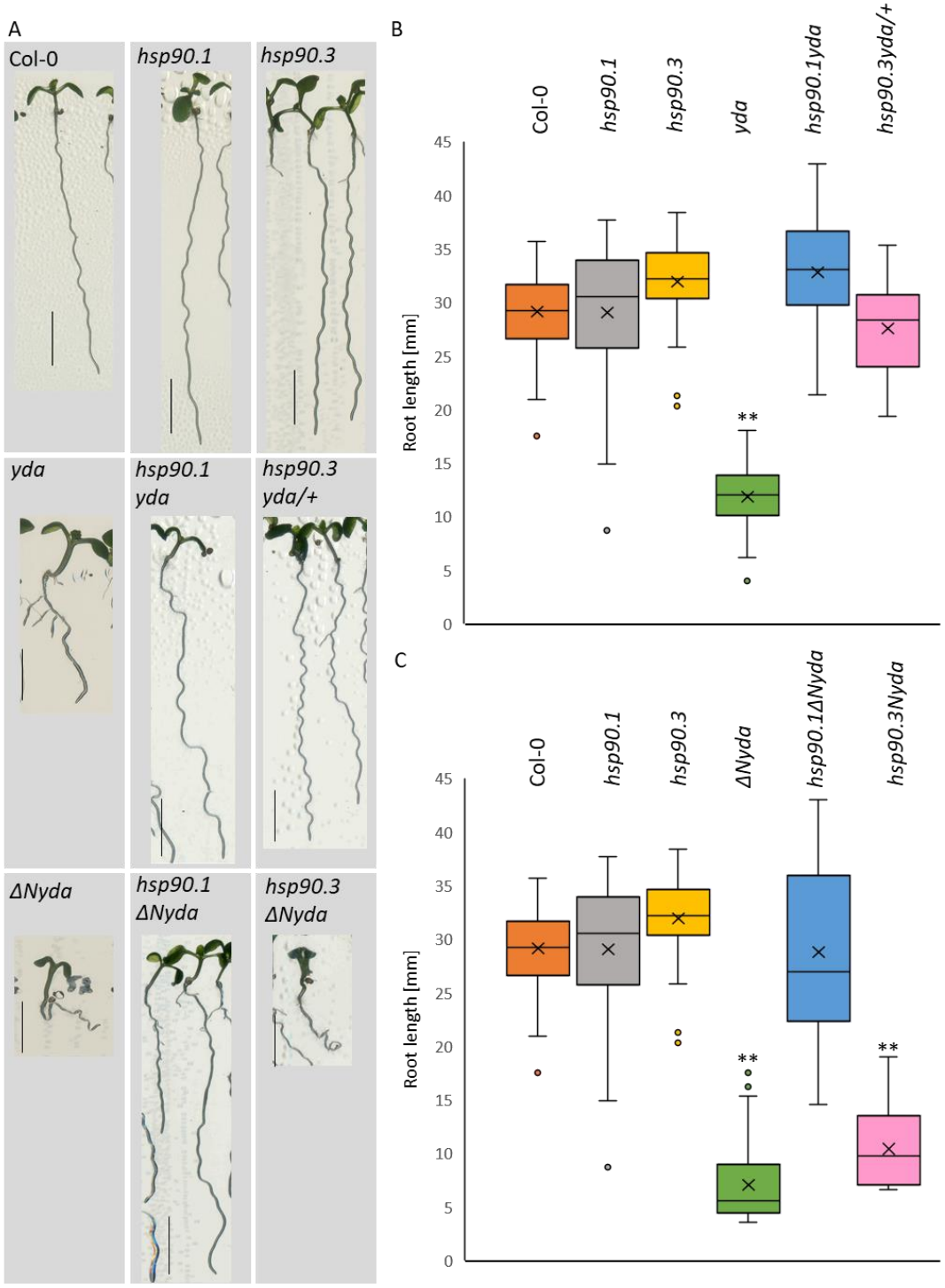

Figure 10: Primary root development in YODA and HSP90 double mutants. Phenotypical (A) observation of root development and statistical measurement of *yda* double mutants (B) and *ΔNyda* double mutants. All measurements show 5 mm. Double asterisk means significant difference from wild-type by p value ($p < 0.01$; Tukey test).

hsp90.3ΔNyda mutant was the only double mutant, which exhibited significantly different phenotype from the wild-type (figure 10A, C). Primary roots were significantly shorter and curved, suggesting that *hsp90.3ΔNyda* root phenotype was comparable to the one of *ΔNyda*. This implies that the *hsp90.3* mutant cannot rescue *ΔNyda* mutant phenotype.

The above results show that HSP90.1 and HSP90.3 have both redundant and differential roles in primary root development, while HSP90.1 seems to have a more distinguished role in root development. We can assume that the HSP90.3 protein is partially replaceable with the HSP90.1 protein, but not on the contrary.

Primary root phenotype of *hsp90.1yda* and *hsp90.1ΔNyda* double mutants showed similar phenotype to the wild-type, but not the *hsp90.3ΔNyda* mutant.

4.1.2 Reproductive phase

To characterize the development of reproductive tissue, we studied the inflorescence formation. We observed the position of emerging buds and flowers where we focused on the size of petals and stigmas.

We used 30 dpg (days post germination) plants of wild-type plants the Col-0 and Ler ecotypes and single and double mutant plants as described above.

To prepare the sample for microscopic analysis, we cut the uppermost 1,5 cm of apical node and placed it on a Petri dish with agarose gel. We prepared at least triplicates for analysis of each of the mutant lines, which were observed from above and sideways using AxioZoom V.16 microscope.

Both *yda* and Δ*Nyda* single mutants exhibited buds closer to each other than in the wild-type (figure 11). The difference in length of the pedicels supporting the bud to the stem was visible when viewed from the side. The pedicels of *yda* and Δ*Nyda* mutants were distinctly shorter, therefore the buds seemed to be more compacted than the ones in the wild type. Moreover, we observed longer carpels in the flowers of both mutants and larger petals in Δ*Nyda* mutant (Figure 11A). In contrast to the YODA mutants, MAPK mutants, *mpk3-1* and *mpk6-2*, exhibited no visible differences in

Figure 11: Floral development of YODA-MAPK signaling cascade single mutants *yda,* Δ*Nyda* (A) and *mpk3-1*, *mpk6-2* (B). Arrows point to longer carpel, arrowheads show larger petals. All measurements show 2 mm.

phenotype from the wild-type (Figure 11B). From these results we can conclude that YODA has a greater effect on flower development and architecture.

Next, we focused on inflorescence development of *hsp90* mutants. None of the three mutant lines *hsp90.1*, *hsp90.3* and *pRac2::hsp90RNAi* showed phenotypic changes compared to the wild-type plants (Figure 12).

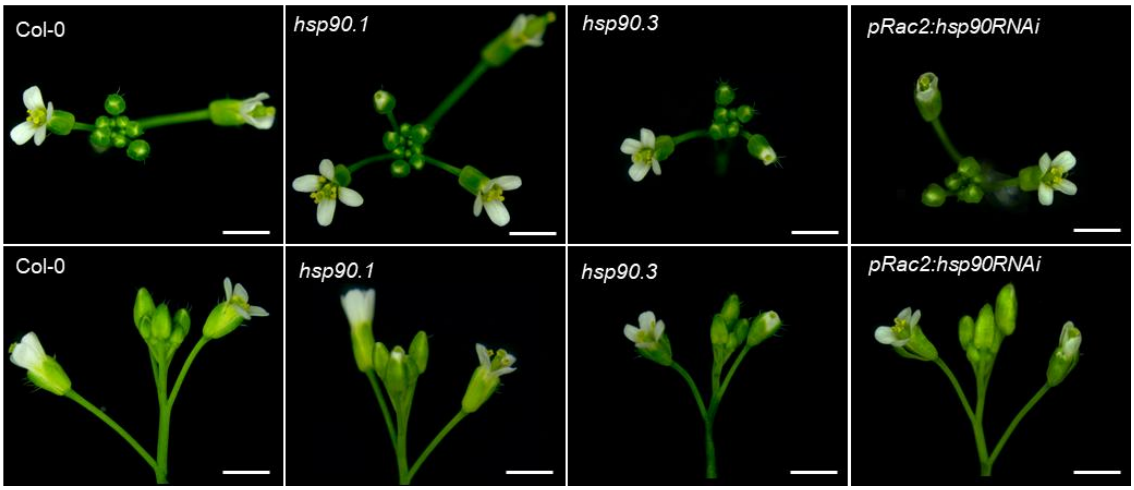

Figure 12: Floral development of *hsp90* mutants. No significant differences between wild-type and mutants are visible. All measurements show 2 mm.

Analysis of flower development and architecture in double mutants showed that none of the double mutants, *hsp90.1yda*, *hsp90.3yda*/+, *hsp90.1*Δ*Nyda* or *hsp90.3*Δ*Nyda*, had wild-type phenotype. Additionally, all of the double mutants differed in the phenotype of inflorescence compared to the *hsp90.1* and *hsp90.3* single mutants. It was also visible that all studied double mutants showed the same phenotypic trait as *yda* and Δ*Nyda* mutants, such as shorter pedicle (Figure 13). Furthermore, *hsp90.3*Δ*Nyda* mutant had one phenotypic trait characteristic for ΔN*yda* mutant, a spike-like structure indicative for arrested flower growth (arrow in Figure 13). This implies that neither *hsp90.1* or *hsp90.3* mutants can completely rescue the inflorescence phenotypes of *yda* or *ΔNyda* mutants.

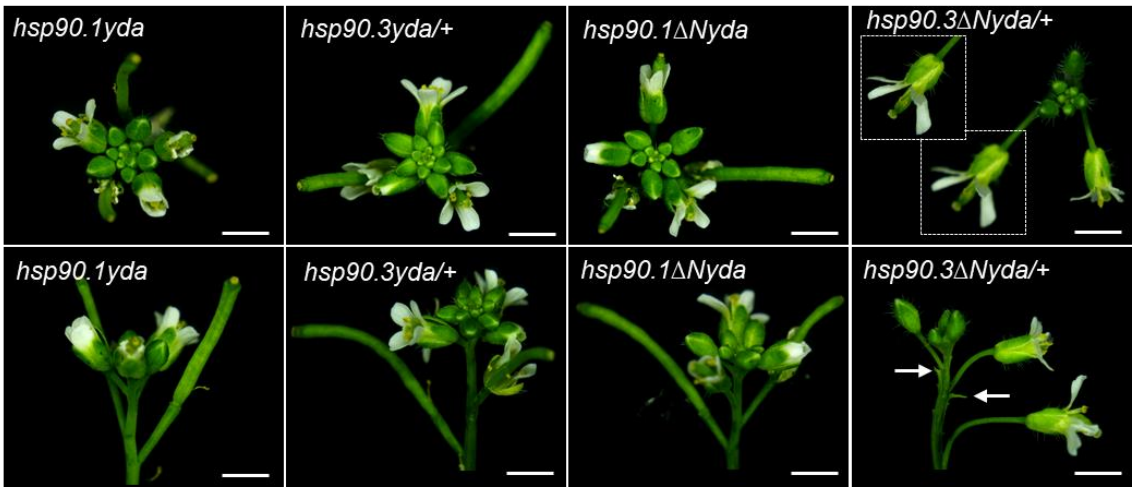

Figure 13: Floral development of HSP90 and YODA double mutants. Compared to the inflorescence of single mutants all double mutants show *yda* or Δ*Nyda* phenotype rather than the phenotype of *hsp90* mutants. Arrow points to spike characteristic for Δ*Nyda* mutant. All measurements show 2 mm.

4.1.3 Early embryo development

To further characterise the impact of YODA-MAPK signaling cascade and HSP90 on the development of a plant, we used embryonic developmental studies, more precisely, the formation of a suspensor and an embryo. Previously published results demonstrated the effect of YDA on embryonic development during the first asymmetric division (Lukowitz *et al.*, 2004). We focused on the interaction of YODA with HSP90 in the characterization of embryogenesis in both single and double mutants.

To visualize embryos, we used the protocol for modified pseudo-Schiff staining with propidium iodide (PI, Truernit et al., 2008). We used the staining of immature seeds with a fluorescent dye (PI) which binds to carbohydrates in the plant cells walls making the observation of individual cell walls between cells possible using a confocal scanning microscope (CLSM). We focused on the early developmental stages of the embryo, especially on the 2- to 4-cell stage and 8-cell stage.

First, we focused on the embryonic development of the wild-type Col-0, which was used as a reference material (Figure 14). Subsequently, we focused on studying simple mutants. Expected number of cells in the suspensor was determined according to the developmental stage of the wild-type embryo (Figure 1). The suspensor of embryo in 2- to 4-cell stage is characteristically divided into two cells (figure 14C). The suspensor of the next developmental stage, the octant, is divided into 4 cells (figure 14D).

Our observation of YODA MAP3K mutants confirmed the previously published results (Lukowitz *et al.*, 2004). We saw distinct defects in the development of *yda* and

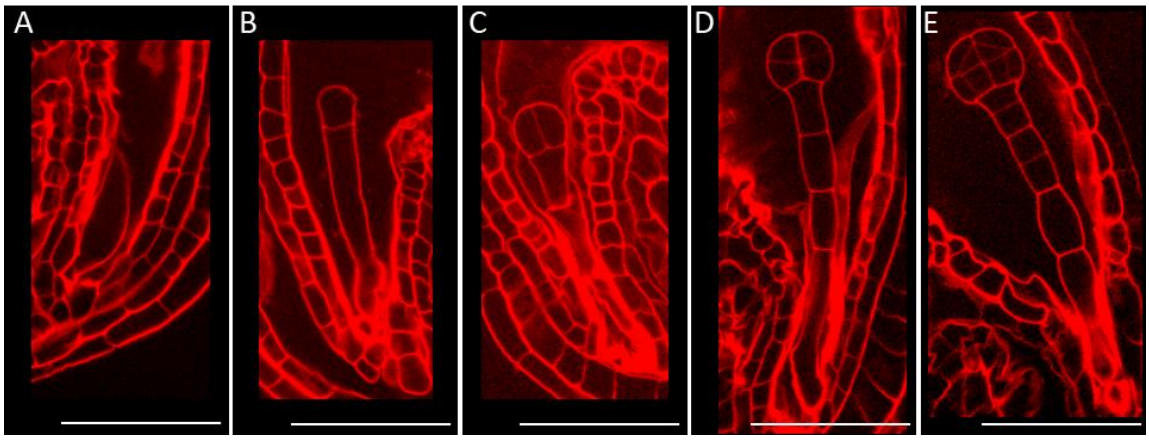

Figure 14: Early embryonic development of Col-0. Early embryogenesis starts from zygote (A) through 1-cell stage (B), 2- to 4-cell stage (C), 8-cell stage (D) and dermatogen (E) inside of embryonic sac. All measurements show 50 μm.

Δ*Nyda* mutants. While *yda* mutants showed a clearly shorter suspensor length and whole embryo was often dwarfed, the length of the Δ*Nyda* suspensor was longer than that of wild type. Development of Δ*Nyda* embryo is hindered by accelerated growth of suspensor. In addition, defects in the orientation of cell divisions appeared in both observed mutants and stages. Atypically oriented cell walls were observed mainly in the embryo, but we also found unusual divisions in the suspensor, leading to abnormal number of cells in suspensor (Figure 15A).

We also observed the development of MAPK mutant embryos, downstream of YDA. Both the *mpk3-1* and *mpk6-2* phenotypes exhibited *yda*-like features, namely the shorter suspensor, which was particularly evident in the earlier developmental stages. We identified misoriented cell division within the 2 cell *mpk3-1* embryo. Surprisingly, we did not find phenotypically unusual embryos at later stages in this mutant. In the case of the *mpk6-2* mutant, the embryos were smaller than the wild-type, but the number of cells in the suspensor did not differ or was higher (2- to 4-cell stage in Figure 15A).

Phenotypic analysis of embryogenesis in *hsp90* mutants revealed mainly misoriented cell divisions in embryo (Figure 15A). The suspensor of *hsp90.1* mutant is usually shorter than in wild-type. Furthermore *hsp90.1* embryo contains unusually oriented cell divisions. The cells in suspensor of *hsp90.3* mutants are shorter and wider than in WT, but the suspensor itself contains more cells. *pRac2::hsp90RNAi* mutants have diverse phenotypes. Some of them have atypical divisions in embryo (e.g. 8-cell stage embryo in the Figure 15A), while others are phenotypically close to the wild type (e.g. 2- to 4-cell stage embryo in the Figure 15A).

Furthermore, we focused on observation of the double mutants. The phenotype of double mutant *hsp90.1yda* has short suspensor, but in contrast to *yda*, the suspensor of double mutant consists of more cells than expected. Embryos are dwarfed and cell walls in dermatogen and later stages are often unrecognisable (data not shown). Surprisingly, we were unable to recognize any atypical phenotypic traits in the *hsp90.3yda/+* embryos. The *pRac2::hsp90RNAiyda* phenotype was variable, especially in the 2-4 cell stage, where we observed embryonic cell extension (figure 15B), but, on the contrary, in the 8-cell stage a longer cell suspensor was observed than what is typical for this stage in wild-type.

The double mutants *hsp90.1*Δ*Nyda*, *hsp90.3*Δ*Nyda* and *pRac2::hsp90RNAi*Δ*Nyda* share similar phenotype. At first, in early stages (up to the 8-cell stage), the suspensor

rapidly elongates (Figure 15B). However, in later stages (dermatogen), the elongation of suspensor seems to stop. Thus, in early stages, the suspensor is as long as in WT or longer, and in later stages, it is shorter than in WT (data not shown).

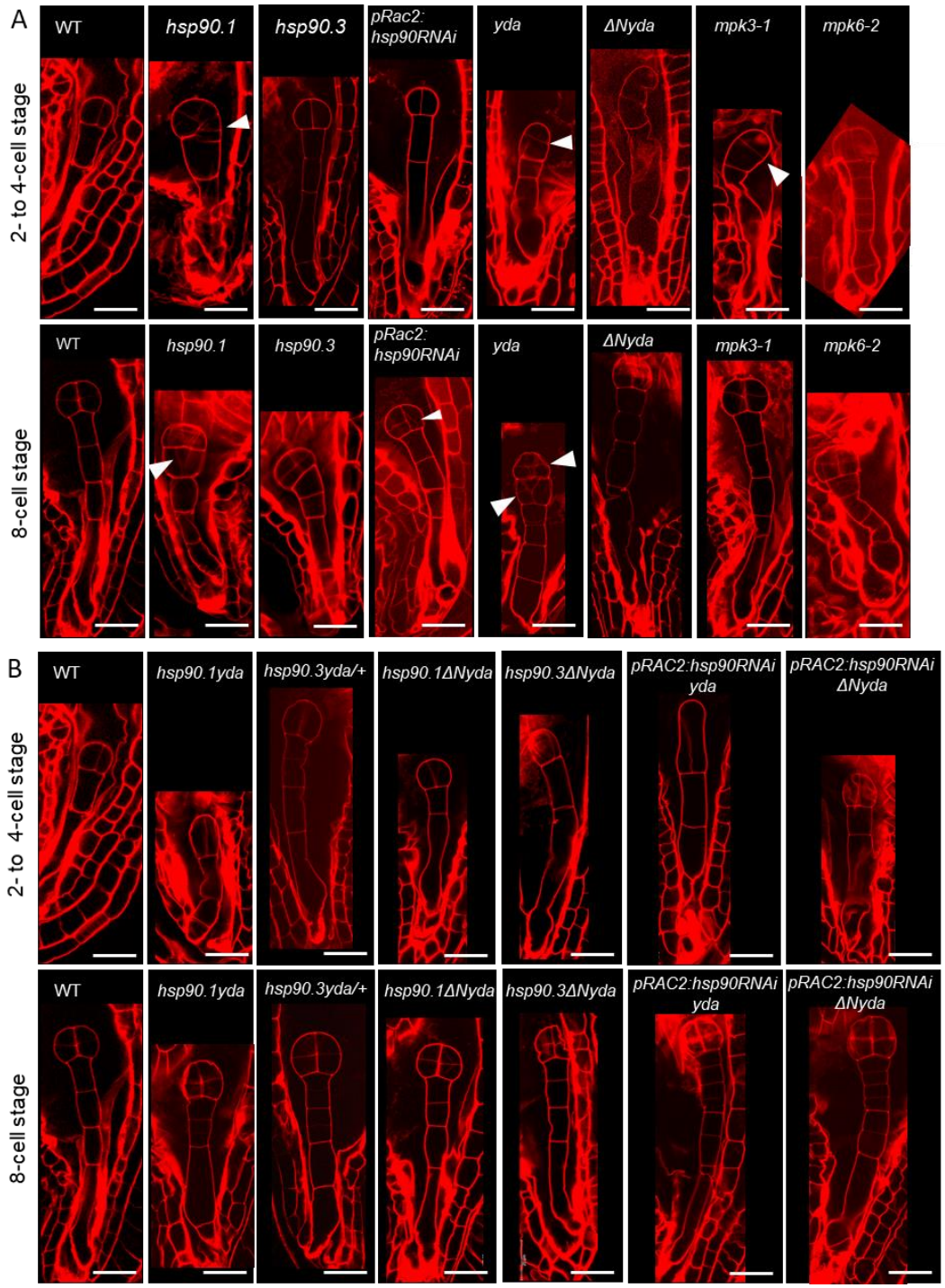

Figure 15: Embryonal development in *hsp90*, *yda* and *mapk* single (A) and double mutants (B). Embryonal development was visualized with propidium iodide staining. Pictures are showing embryos in: 2-cell, respectively 4-cell stages (distinguishing between these stages is unreliable); and octant, respectively dermatogen, stages. White arrowheads point to wrongly positioned cell walls, all measurements show 20 µm.

In addition, both *pRac2::hsp90RNAiyda* and *pRac2::hsp90RNAiΔNyda* mutants have the same phenotypic trait, the number of cells in the suspensor at 8-cell stage is increased. This phenotypical trait is not visible in other *hsp90* double mutants.

From these results we conclude, that there are no defects in cell division plane orientation during early embryonal development in any of presented double mutants. Moreover, embryos (not suspensors) did not differ significantly from wild type phenotypes. We can therefore claim, that we have observed both *hsp90.1* and *hsp90.3* to partially rescue *yda* or Δ*Nyda* phenotype.

4.2 Western blot analysis for HSP90, MPK3/6 protein levels and MPK3/6 phosphorylation

To study changes in the protein levels we analyzed protein abundance in the *hsp90.1, hsp90.3, pRac2::hsp90RNAi, mpk3-1* and *mpk6-2* single mutants. Specifically, we focused on protein abundance of both phosphorylated and unphosphorylated forms of MPK3 and MPK6 proteins and protein levels of HSP90 family.

Since we focused on HSP90 YODA cascade interplay during embryonic development, we extracted proteins from young developing siliques. We made two biological repetitions of the experiment, each consisting of three technical replicates.

Samples with the same protein concentration were resolved by polyacrylamide gel electrophoresis. Then, proteins were transferred to PVDF (Polyvinylidene difluoride) membrane where immunoblot analysis was performed by using specific antibodies. For the detection of the phosphorylated forms of MPK3/6 kinases we used pERK antibody that can bind to the phosphorylated motif of MPK3/6 (Figure 16).

Analysis of the protein levels of MPK3 showed significant difference in protein abundance in all mutants (Figure 17A). MPK3 protein levels were significantly lower in *hsp90.1, hsp90.3, pRac2::hsp90RNAi* and *mpk6-2* mutants that in wild-type. In the case of MPK6, no significant difference in abundance was detected in any mutant.

In addition, we examined the abundance of phosphorylated, thus activated, MAPK (Figure 17B). The phosphorylated form of MPK3 (pMPK3) showed a similar trend to

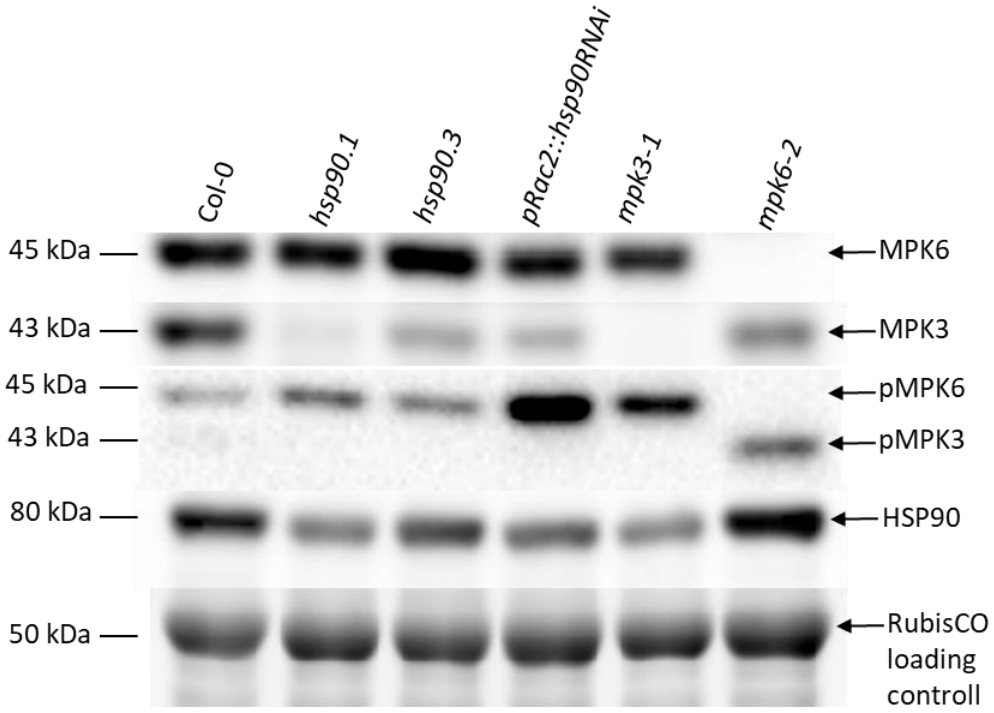

Figure 16: Cutouts of western blots images. From the top membrane was used specific primary antibody anti-MPK6, anti-MPK3, anti-pTEpY and HSP90. The bottom view shows RubisCO as a loading control. The approximate molecular weights of the studied proteins were estimated according to the marker and they are assigned to each band on the left. On the right, the arrows indicate a horizontal plane where the bands of labeled proteins are located.

its non-phosphorylated form. In *hsp90* mutants pMPK3 abundance decreased, with *hsp90.1* and *hsp90.3* showed a statistically significant decrease of pMPK3 abundance compared to wild type. *pRac2::hsp90RNAi* mutant did not exhibit statistically significant decrease of pMPK3. In contrast the mutant *mpk6-2* showed the opposite trend, the abundance of pMPK3 was significantly increased compared to wild-type. The phosphorylated form of the MPK6 enzyme (pMPK6) was significantly increased in *hsp90.1*, *pRac2::hsp90RNAi* and in *mpk3-1*. No significant difference was observed in the levels of pMPK6 in *hsp90.3* mutant (Figure 17B).

Regarding both the total amount of phosphorylated and non-phosphorylated forms of MAPK (Figure 17C), the results support observations in individual forms. The total amount of MPK3 was significantly reduced in *hsp90* mutants, while the amount of MPK6 was increased in these mutants. The statistically significant difference in total MPK6 protein level was confirmed in the *hsp90.1* and *pRac2::hsp90RNAi* mutants, but not in *hsp90.3*. The total amount of MPK6 was mildly increased in *mpk3-1*, but not significantly.

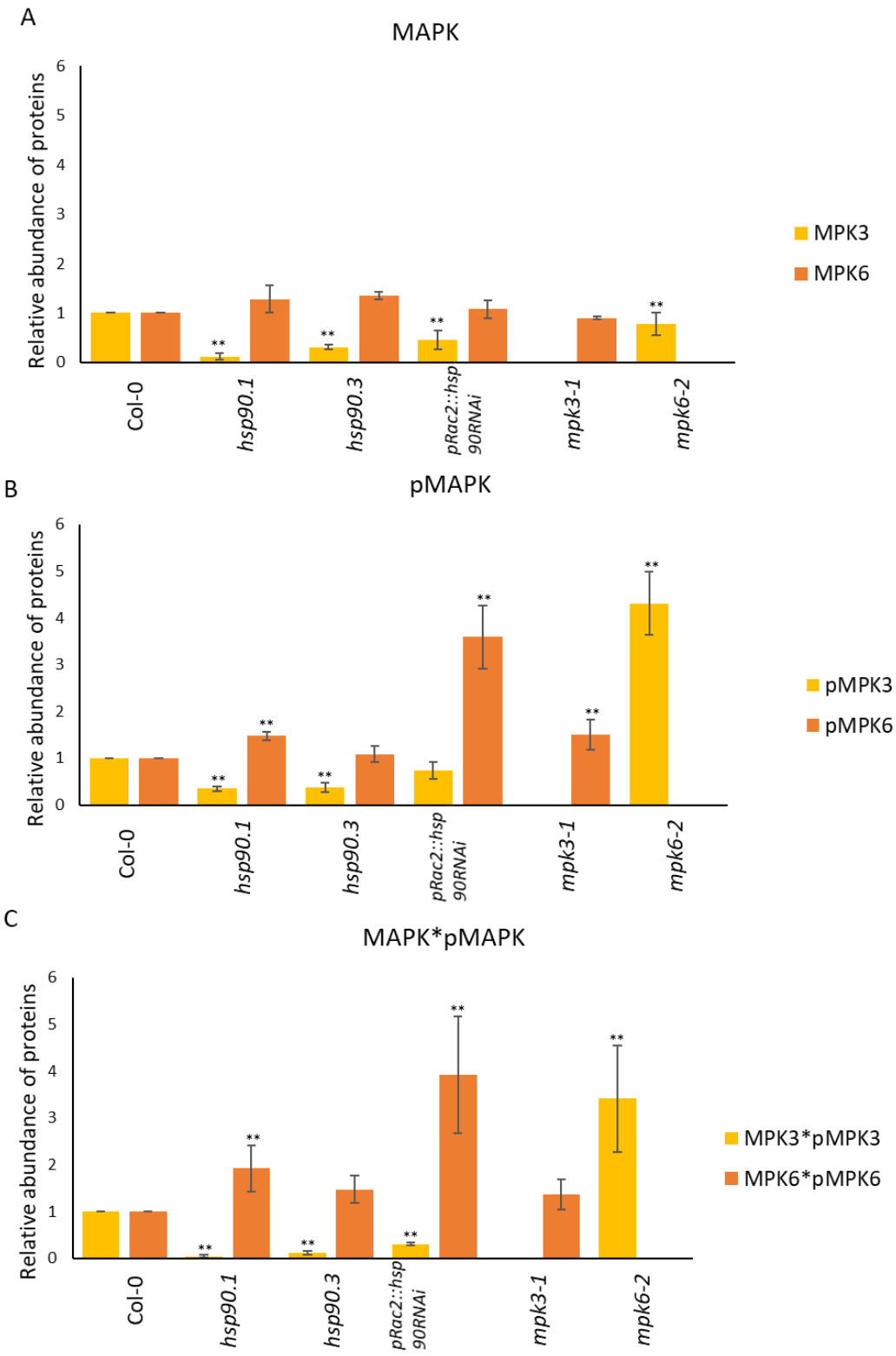

Figure 17: Relative abundance of MPK3 and MPK6 proteins. Graphs show comparison of MPK3 and MPK6 protein abundance in siliques of wild-type plants and studied mutants. Analysis of MAPKs' unphosphorylated forms (A), phosphorylated forms (B) and both (C) were performed. Abundance of proteins in mutants were compared to protein levels in wild type. Double asterisk points out significant difference compared to the wild-type (ANOVA followed by Tuckey HSD test, $p < 0,01$).

Conversely, total MPK3 abundance was significantly decreased in all *hsp90* mutants (*hsp90.1*, *hsp90.3* and *pRac2::hsp90RNAi)* and, on the contrary, significantly increased in the *mpk6-2* mutant.

In *mpk3-1* mutant we did not detect any presence of MPK3 or pMPK3 as well as in *mpk6-2* mutant we did not detect any MPK6 or pMPK6 (Figure 17A to C). On the other hand, in *mpk3-1* mutant was increased abundance of MPK6 and *mpk6-2* mutant show increased protein level of MPK3 (Figure 17A to C). This observation suggests, that the functions of these two kinases are partially overlapping and when one is missing, its function is partially replaced by the other. It is apparent from the graph, that the amount of pMPK6 and the total abundance of MPK6 in *mpk3-1* is lower than protein level of pMPK3 and the total MPK3 in *mpk6-2*.

In conclusion, both *hsp90.1* and *hsp90.3* mutants exhibit a significant reduction in abundance of both phosphorylated and non-phosphorylated forms of MPK3. On the other hand, *hsp90* mutants show an increase in both forms of MPK6, however, this is statistically significant only in *hsp90.1* and *pRac2::hsp90RNAi*.

The relative abundance of HSP90 family proteins was significantly reduced in the *hsp90.1*, *hsp90.3*, *pRac2::hsp90RNAi* and *mpk3-1* mutants (Figure 18). In contrast, *mpk6-2* exhibited mild, but not statistically significant, increase in HSP90 abundance. This suggests that both kinases are regulated by HSP90 proteins.

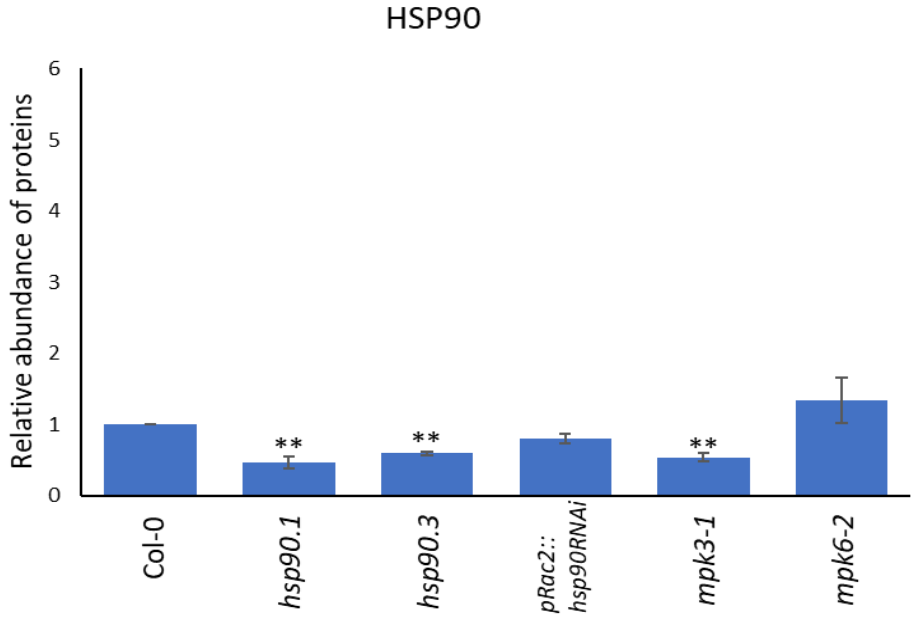

Figure 18: Relative abundance of HSP90 proteins. Graph shows comparison of HSP90 protein abundance in siliques of wild-type plants and in siliques of studied mutants. Double asterisk points on significant difference compared to the wild-type. To analyse significant difference we used ANOVA and Tuckey tests with p value $p < 0,01$.

4.3 Analysis of WOX8 expression pattern in hsp90 and YODA cascade mutants.

Expression of the WOX8 is activated by YODA-MAPK cascade. Through YDA cascade MPK3 and MPK6 kinases are phosphorylated, which in turn activate by phosphorylation WRKY2 transcription factor, which than initiates WOX8 transcription (Ueda *et al.,* 2017). To further study the YODA-MAPK cascade mutants and *hsp90* mutants, we focused on expression pattern of WOX8 transcription factor. Therefore, we studied the WOX8 expression in wild-type, *yda*, Δ*Nyda*, *mpk3* and *mpk6* mutants as well as in *hsp90.1* and *hsp90.3* mutants.

4.3.1 Selection of homozygous mutant plants by PCR and electrophoresis

In order to obtain mutant lines expressing the *pWOX8::NLS:YFP* construct, we crossed single mutants *yda*, Δ*Nyda*, *mpk3-1*, *mpk6-2*, *hsp90.1* and *hsp90.3* with the *pWOX8::NLS:YFP* reporter line. After self-pollination of genetically uniform F1 plants we harvested seeds. These F2 seeds were plated on Petri dishes. To select T-DNA insertion homozygous plants PCR analysis of seedlings was performed. We used primers specific for genes of interest and for inserted T-DNA (Table 1 and 2 in methods). Furthermore, microscopic observation was performed only with plants homozygous for T-DNA insertion in the gene of interest, with the exception of *yda*, Δ*Nyda* which are fertile only in heterozygous state. Due to the strong phenotype of *yda* and Δ*Nyda*, we were able to select mutant embryos during microscopic analysis.

First, we searched for homozygous mutants for *mpk3-1* (Figure 19) and *mpk6-2* (Figure 20). Secondly, we focused on the *hsp90.1* (Figure 21) and *hsp90.3* (Figure 22) mutants. We also performed PCR analysis for the *yda* and Δ*Nyda* mutants (data not shown). Since the PCR analysis is prone to technical problems (Figure 22), each putative homozygot was confirmed by two more independent PCR, thus for the genotyping, technical triplicates were performed.

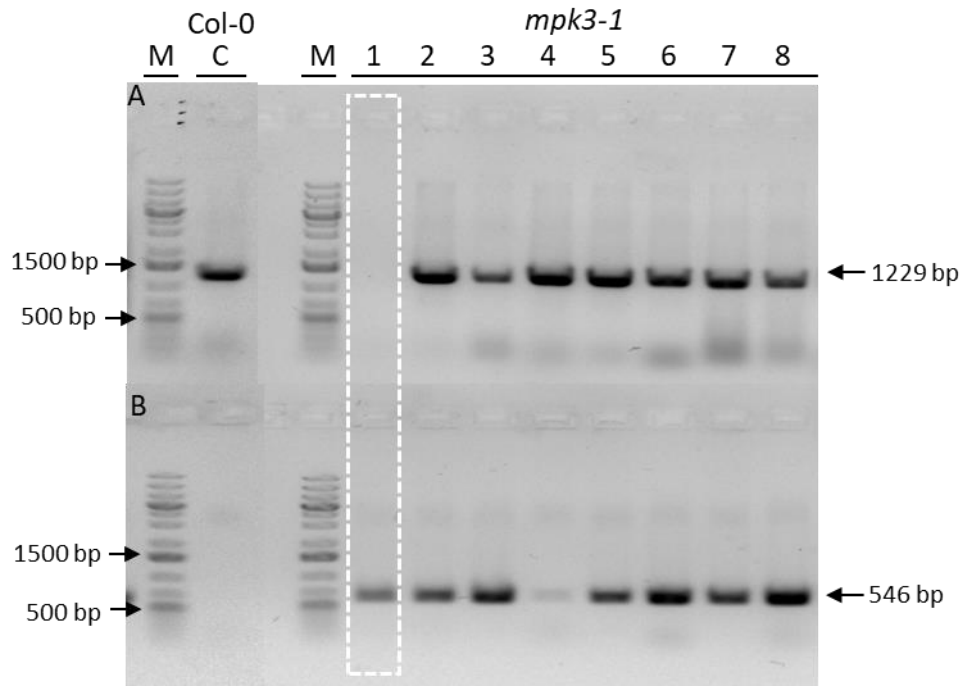

Figure 19: Agarose gel electrophoresis with PCR products amplified with primers for *MPK3* gene (A) and T-DNA insertion in *MPK3* gene (B). The position on gel in both (A) and (B) is: (M) – marker, (C) control – wild type, (1-8) samples from *mpk3-1pWOX8::NLS:YFP* F2 generation. Samples 2-8 represent heterozygous plants with one wild-type allele and one allele with T-DNA insertion. Sample 1 is homozygous for T-DNA insertion (white rectangle). PCR product for *MPK3* gene is 1229 bp long and for T-DNA insertion in *MPK3* gene it is 546 bp long.

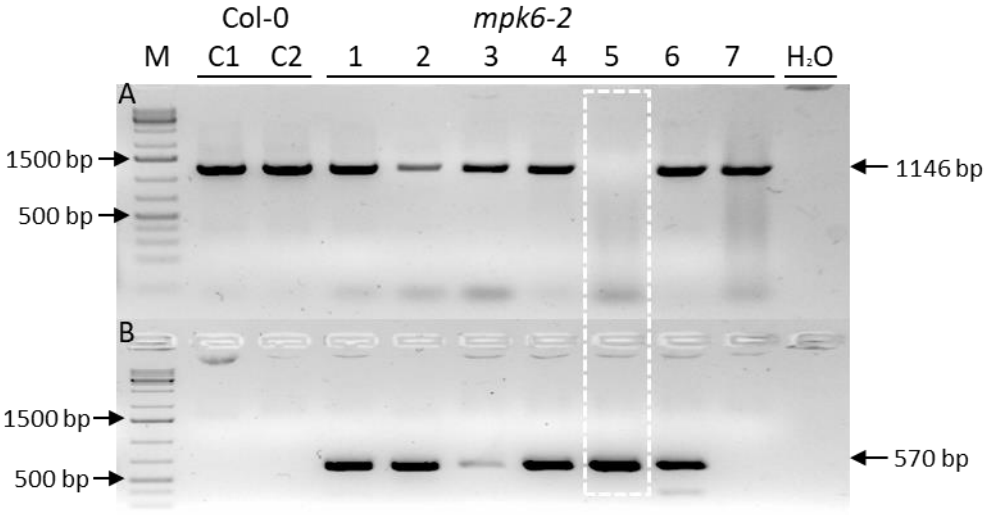

Figure 20: Agarose gel electrophoresis with PCR products amplified with primers for *MPK6* gene (A) and T-DNA insertion in *MPK6* gene (B). The position on gel in both (A) and (B) is: (M) – marker, (C1, C2) control – wild type, (1-7) samples from *mpk6-2pWOX8::NLS:YFP* F2 generation, (H2O) - negative control. Samples 1 to 4 and 6 represent heterozygous plants with one wild-type allele and one allele with T-DNA insertion. Sample 7 is a wild type. Sample 5 is homozygous for T-DNA insertion (white rectangle). PCR product for *MPK6* gene is 1146 bp long and for T-DNA insertion in *MPK6* gene it is 570 bp long.

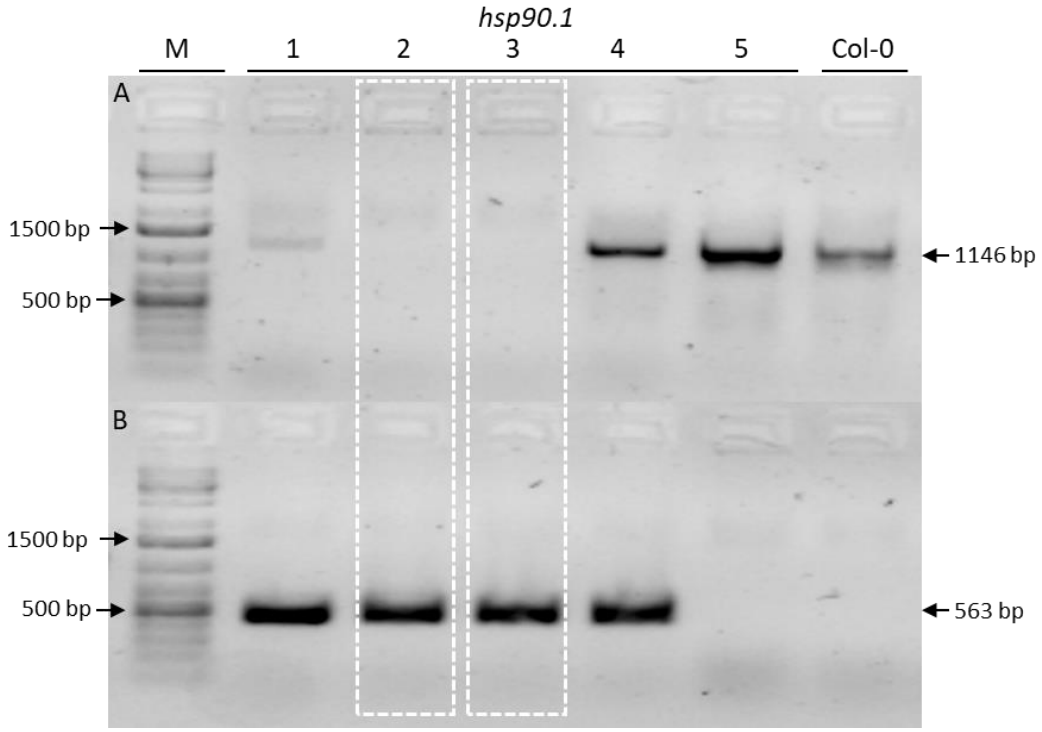

Figure 21: Agarose gel electrophoresis of PCR products amplified with primers for *HSP90.1* gene (A) and T-DNA insertion in *HSP90.1* gene (B). The position on gel in both (A) and (B) is: (M) – marker, (1-5) samples from *hsp90.1pWOX8::NLS:YFP* F2 generation, (C) – control – wild type. Samples 1 and 4 represent heterozygous plants with one wild-type allele and one allele with T-DNA insertion. Samples 2 and 3 are homozygous for T-DNA insertion (white rectangle). Sample 5 is wild type. PCR product for *HSP90.1* gene is 1146 bp long and for T-DNA insertion in *HSP90.1* gene it is 563 bp long.

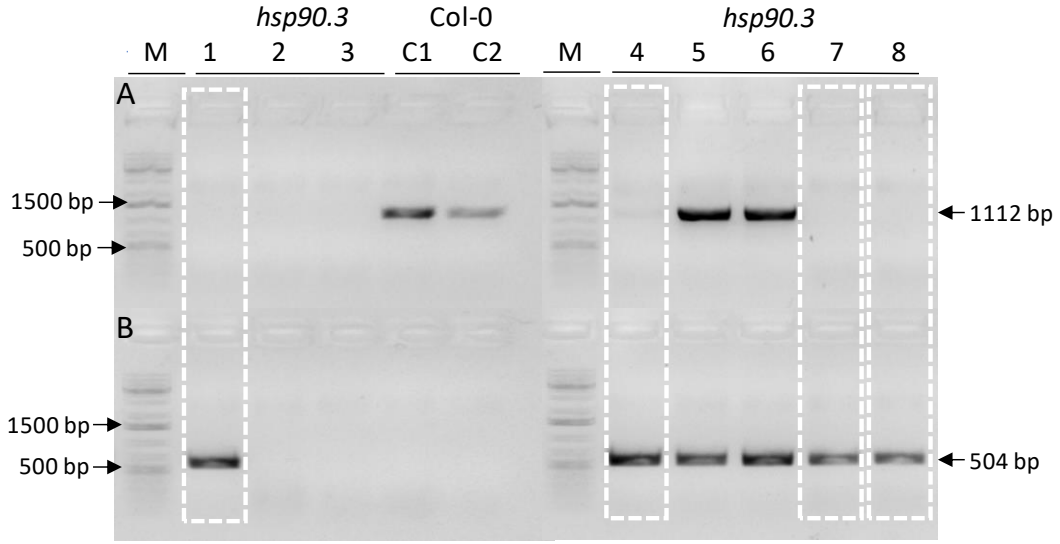

Figure 22: Agarose gel electrophoresis of PCR products amplified with primers for *HSP90.3* gene (A) and T-DNA insertion in *HSP90.3* gene (B). The position on gel in both (A) and (B) is: (M) – marker, (1-3) samples from *hsp90.3pWOX8::NLS:YFP* F2 generation, (C1, C2) – control – wild type, (4-8) samples. Samples 5 and 6 represent heterozygous plants with one wild-type allele and one allele with T-DNA insertion. Samples 1, 4, 7 and 8 are homozygous for T-DNA insertion (white rectangle). PCR reaction for samples 2 and 3 did not work..PCR product for *HSP90.3* gene is 1112 bp long and for T-DNA insertion in *HSP90.3* gene it is 504 bp long.

4.3.2 Microscopic observation of *pWOX8::NLS:YFP* construct

As mentioned in the theoretical part, WOX8 is transcription factor specifically expressed in the suspensor cells of the developing embryo. We analyzed changes in suspensor development using mutants carrying the *pWOX8::NLS:YFP* construct. We characterized the WOX8 expression pattern in these mutants. We worked with the *pWOX8::NLS:YFP* reporter line and *ydapWOX8::NLS:YFP*, *ΔNydapWOX8::NLS:YFP*, *mpk3-1pWOX8::NLS:YFP*, *mpk6-2pWOX8::NLS:YFP*, *hsp90.1pWOX8::NLS:YFP*, *hsp90.3pWOX8::NLS:YFP* single mutants. To statistically evaluate microscopic observations, we counted embryos with missing signal in suspensor cells and embryos with ectopic signal in embryo proper (the area surrounding embryo).

By observing embryonic development in wild-type by mPS-PI (Truernit et al., 2008) we confirmed the typical number of cells in the suspensor for individual developmental stages of embryo. To confirm whether we have correctly characterized the number of suspensor cells in various stages of development, we examined the expression of the inserted construct *pWOX8::NLS:YFP* in wild-type embryos. The WOX8 promoter provides tissue-specific expression of the construct in suspensor cells.

Both methods, mPS-PI and expression of WOX8, lead to the same results, namely that the suspensor of 2-cell stage embryo has 2 cells (Figure 23A) and after next division in embryo resulting in 4-cell embryo there are 3 cells in suspensor (Figure 23B). The suspensor of the following developmental stage, the octant, consists of 4 cells (Figure 23C) and in globular stage, the suspensor is divided into 6 or more cells (Figure 23D).

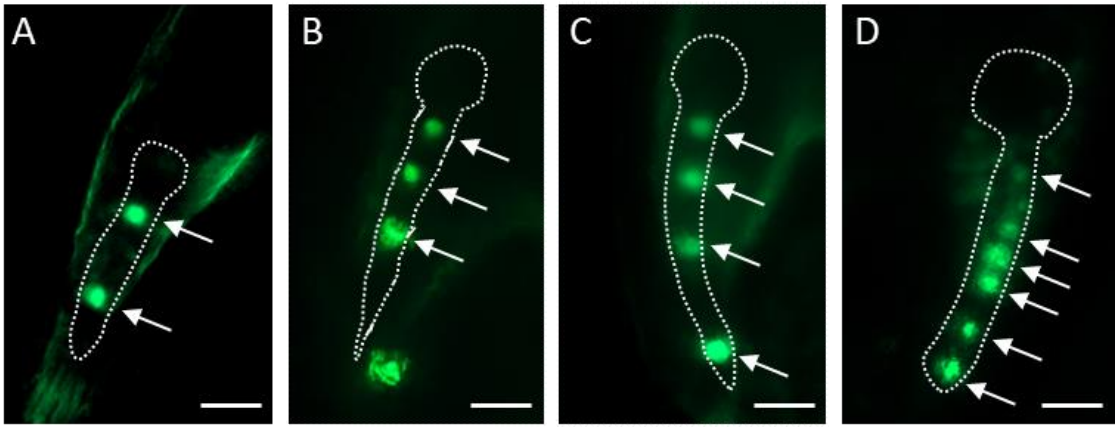

Figure 23: Expression of WOX8 transcription factor during early embryo development. Arrows highlight the nuclei of the suspensor cells at the 2-cell stage (A), 4-cell stage (B), octant (C) and globular stage (D) of embryo development. All measurements show 20 μm.

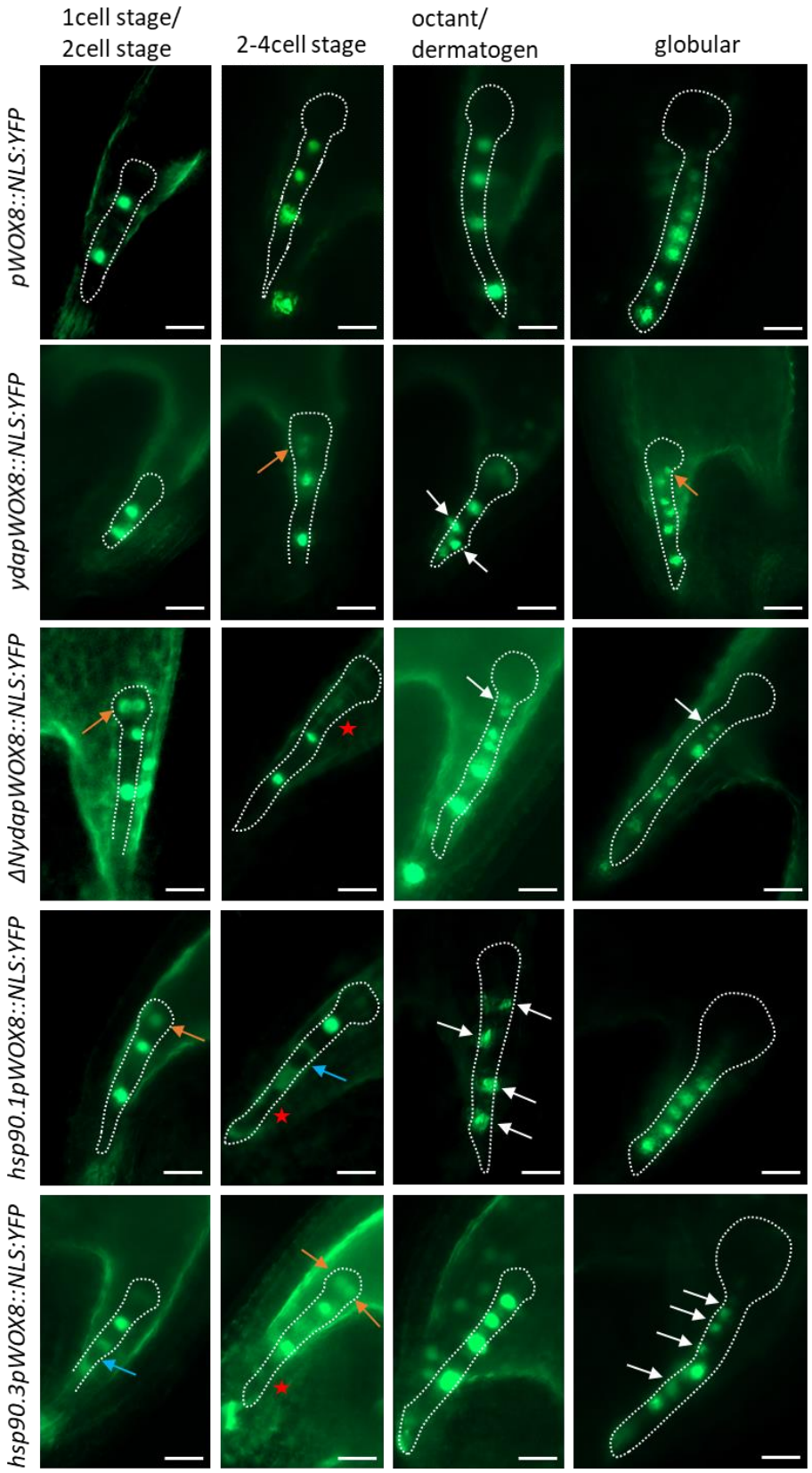

Figure 25: Embryonic development and expression of WOX8 transcription factor in wild type, *yda*, Δ*Nyda* and *hsp90* mutants. White arrows point to weaker signal in nucleus of suspensor cells, orange arrows point to ectopic signals in embryo, blue arrows pointed to signal in cell outside of nucleus and red stars next to suspensor indicate missing signal in suspensor. All measurements show 20 μm.

Expression analysis of WOX8 in the severely defective *yda* embryos showed ectopic expression in the apical part of the embryo (indicated by the orange arrow in Figure 24, 25), while the nuclei in suspensor cells are not aligned like in the wild-type embryos suggesting irregular cell divisions (Figure 24, dermatogen stage). In contrast, Δ*NydapWOX8::NSL:YFP* exhibited more frequently missing signal in suspensor (Figure 24, 2-4 cell stage; 25). In some cases, the YFP signal could not be focused to one clearly defined spot (Figure 24, dermatogen stage). We also observed very weak signal (Figure 24, globular white arrows). In addition, we observed signals in close proximity, which may indicate a large number of divisions in suspensor that result in small cells (Figure 24, octant). We also observed an atypical signal in nucleus of embryonic cells (Figure 24, 2-cell stage).

We also studied the expression of the WOX8 transcription factor in *hsp90* mutants. In the suspensor cells of *hsp90.1pWOX8::NSL:YFP* signal was atypically distributed. In some cells the signal was completely absent (Figure 24, 1 or 2 cell stage; 25) or it was localized in the cytoplasm instead of the nucleus (Figure 24, 2-4 cell stage). We also observed signals that were not aligned like in the wild-type embryos suggesting irregular cell divisions (Figure 24, octant). Weak fluorescent signal in *hsp90.3pWOX8::NSL:YFP* was detected in embryo (Figure 24, 2-4 cell stage), where

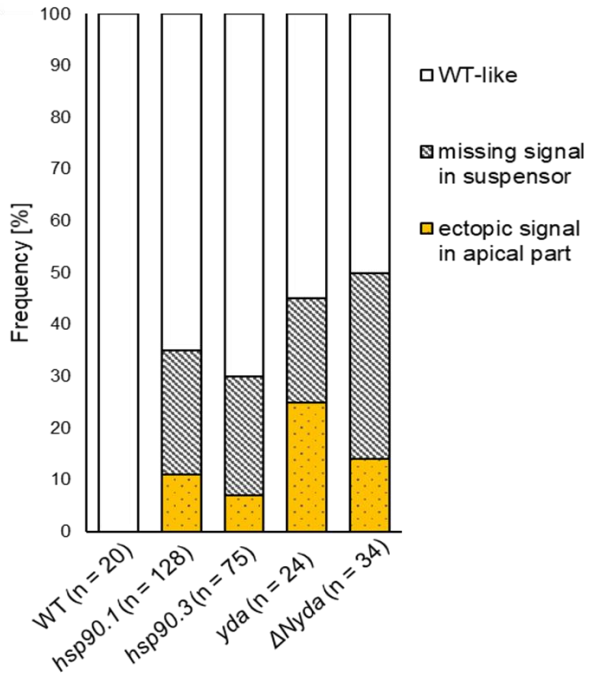

Figure 25: Quantitative analysis of atypical *pWOX8::NLS:YFP* signal localization in the *yda*, Δ*Nyda* and *hsp90* mutants compared to wild type (n = number of observed embryos).

the signal is ectopic. Overall, signal intensity and distribution in the suspensor cells of this mutant are highly variable. In some mutants, very strong signals are observed in the cells of the suspensor (Figure 24, octant stage), sometimes the signal is very weak (Figure 24, white arrows) or as in *hsp90.1pWOX8::NSL:YFP* it is not in the cell nucleus but in the cytoplasm (Figure 24, 1 or 2 cell stage).In *mpk3-1pWOX8::NSL:YFP* we observed weak signal in the upper part of the suspensor (Figure 26, 2-4 cell stage and globular stage; 27). Also, signal was observed in the embryo proper or on the border between the embryo and the suspensor (Figure 26, dermatogen stage). In the *mpk6-2* mutant were observed more signals in suspensor than expected (Figure 26; 27), suggesting a greater number of cells in the suspensor

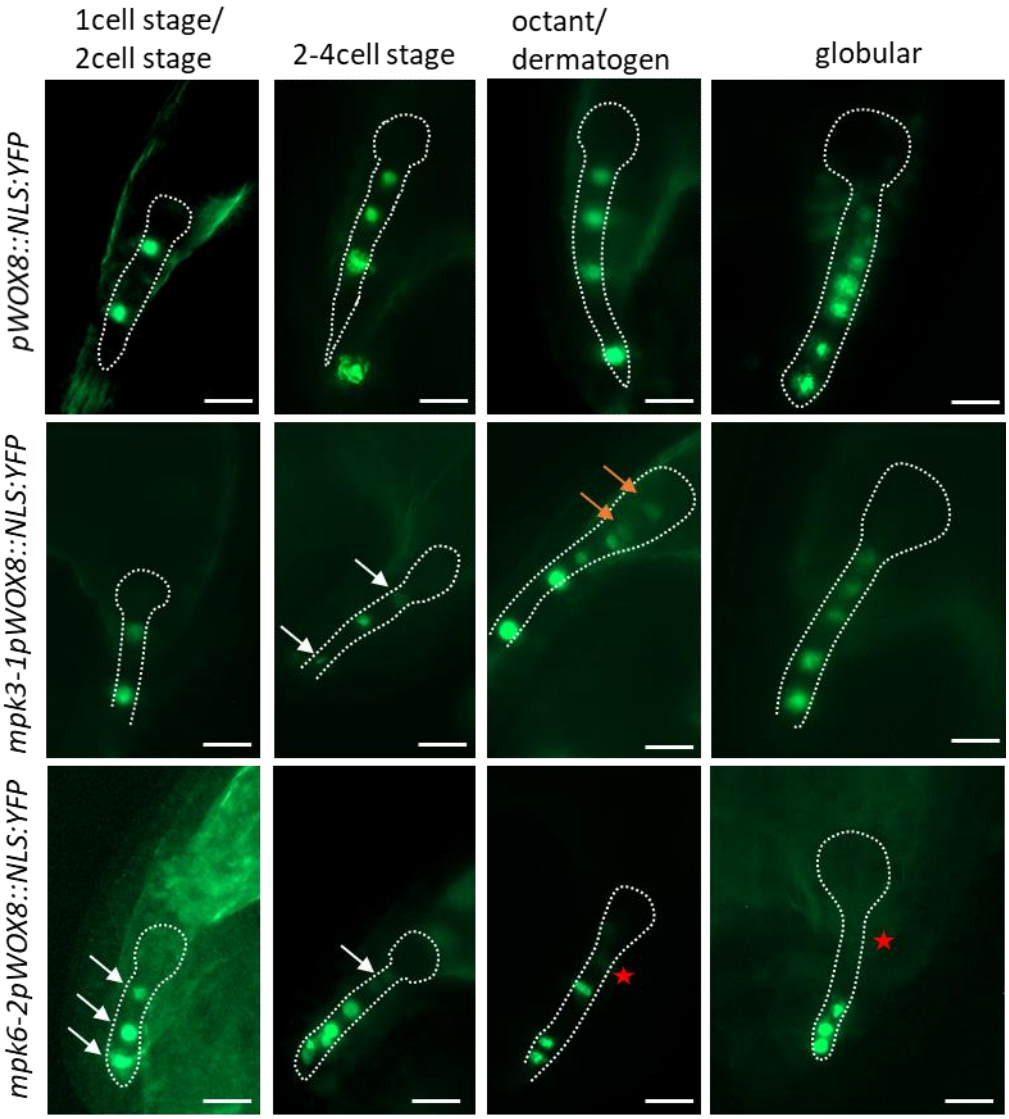

Figure 26: Embryonic development and expression of WOX8 transcription factor in wild type, *yda*, Δ*Nyda* and *hsp90* mutants. White arrows point to weaker signal in nucleus of suspensor cells, orange arrows point to ectopic signal in embryo and red stars next to suspensor indicate missing signal in suspensor. All measurements show 20 μm.

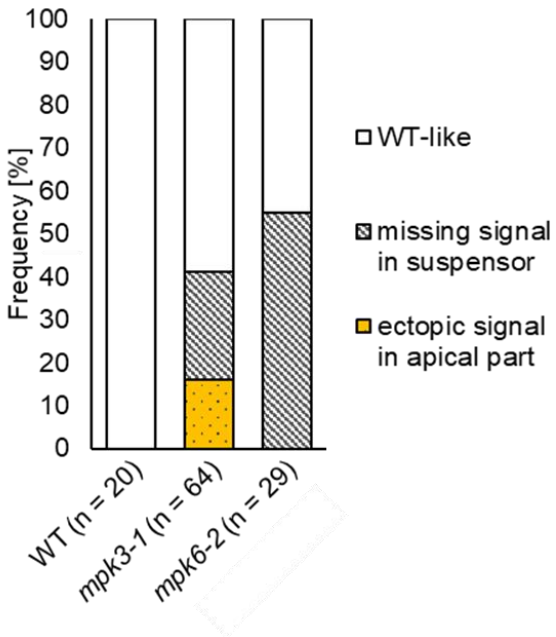

Figure 27: Quantitative analysis of atypical *pWOX8::NLS:YFP* signal localization in the *yda*, Δ*Nyda* and *hsp90* mutants compared to wild type (n = number of observed embryos).

than is typical for the same embryo stage of wild type (Figure 26, 2-cell stage). Similarly to *mpk3-1*, in some cells the signal was weaker than in wild-type suspensor, or the signal was completely absent (Figure 25). On the contrary, we did not observe any ectopic signals in cells of embryo (Figure 27).

Microscopic observation confirmed that a fluorescent signal under the native promoter for the WOX8 transcription factor is untypically expressed in both suspensor and embryo cells of mutants. To conclude all these results, we provide evidence that both YDA-MAPK cascade, namely MPK3 and MPK6, and protein family HSP90 significantly affect establishing of suspensor and embryo cell fates cell divisions in suspensor. Extending the study to double mutants would confirm that the proteins are linked to one signaling pathway.

5 Conclusion

The main aim of this thesis was to characterize the embryonic development of single and double mutants in the HSP90 and YODA-MAPK cascade. For this purpose, we focused on development of the primary root of seedlings and subsequently on the development of inflorescence as a reproductive organ, followed by observation of early embryogenesis. Furthermore, we examined the expression of the suspensor-specific transcription factor WOX8 in the studied single mutants. The following conclusions were drawn from the results of each experiment:

1. We confirmed that the YODA-MAPK cascade has a major influence on the embryonic development, inflorescence architecture and formation of the primary root. In two of these cases, we found out that HSP90 protein family interacts with YODA-MAPK cascade as proved by observing partial rescue in double mutants.
2. Regarding primary root length, the *hsp90.1yda*, *hsp90.1*Δ*Nyda*, and *hsp90.3yda* double mutants exhibited partial rescue in this trait.
3. The development of inflorescence as a reproductive organ is also influenced by the YODA-MAPK cascade, however, the phenomenon of partial rescue was not observed for the double mutants, although single *hsp90* mutants did not differ phenotypically from the wild-type.
4. Early embryogenesis is significantly affected by YODA-MAPK cascade and HSP90 family. Abnormal embryonic development was observed in all single and double mutants. Importantly, single mutants showed severe problems in cell division plane orientation, while similar phenotype was not observed in any of the double mutants. Rescue in this trait provides genetic evidence for interaction between HSP90 and YODA-MAPK cascade in early embryonic development.
5. Analysis of protein levels of HSP90 and phosphorylated as well as non-phosphorylated MPK3 and MPK6 kinases by western blotting demonstrated change in proteins levels in single mutants. Functions of MPK3 and MPK6 are partially overlapping and abundance of both kinases are regulated by HSP90.
6. Observation of WOX8 expression in single mutants showed abnormal expression patterns. These changes correlate with those observed in early

embryogenesis with mPS-PI. This finding further emphasizes the role of YODA-MAPK cadscade in embryogenesis.

After summarizing these results, we can conclude that embryonic development is affected by both HSP90 and YODA-MAPK cascade proteins. Furthermore, we can also say that these two components influence each other and are important for normal plant development.

6 References

ANOVA: http://astatsa.com/OneWay_Anova_with_TukeyHSD 2.3.2019

Balczun C., Bunse A., Schwarz C., Piotrowski M., Kuck U. (2006): Chloroplast heat shock protein Cpn60 from Chlamydomonas reinhardtii exhibits a novel function as a group II intron-specific RNA-binding protein. *FEBS Letters* **580**, 4527-4532.

Bayer M., Nawy T., Giglione C., Galli M., Meinnel T., Lukowitz W. (2009): Paternal control of embryonic patterning in *Arabidopsis thaliana*. *Science* **323**, 1485-1488.

Bayer M., Slane D., Jürgens G. (2017): Early plant embryogenesis: dark ages or dark matter? *Current Opinion in Plant Biology* **35**, 30-36.

*Beere H.M., Wolf B.B., Cain K., Mosser D.D., Mahboubi A., Kuwana T., Tailor P., Morimoto R.I., Cohen G.M., Green D.R. (2000): Heat-shock protein 70 inhibits apoptosis by preventing recruitment of procaspase-9 to the Apaf-1 apoptosome. Nature Cell Biology **2**, 469-475.*

Berardini TZ, Bollman K, Sun H, Poethig RS. 2001. Regulation of vegetative phase change in Arabidopsis thaliana by cyclophilin 40. *Science* **291**, 2405–2407.

Bergmann D.C., Lukowitz W., Somerville C.R. (2004): Stomatal development and pattern controlled by a MAPKK kinase. *Science* **304**, 1494-1497.

Boscá S., Knauer S., Laux T. (2011): Embryonic development in Arabidopsis thaliana: from the zygote division to shoot meristem. *Frontiers in Plant Science* **2**, 18-26.

Boscá S., Knauer S.,Laux T. (2011): Embryonic development in *Arabidopsis thaliana*: from the zygote division to the shoot meristem. *Frontiers in Plant Science* **2**, 1-6.

Bukau B., Horwich A.L. (1998): The Hsp70 and Hsp60 chaperone machines. *Cell* **92**, 351-366.

Calderini, O., Bogre, L., Vicente, O., Binarova, P., Heberle-Bors, E., and Wilson, C. (1998). A cell cycle regulated MAP kinase with a possible role in cytokinesis in tobacco cells. *Journal of Cell Science* **111**, 3091–3100.

Colcombet J., Hirt H. (2008): *Arabidopsis* MAPKs: a complex signalling network involved in multiple biological processes. *Biochemical Journal* **413**, 217-226.

Costa L.M., Marshall E., Tesfaye M., Silverstein K.A.T., Mori M., Umetsu Y., Otterbach S.L., Papareddy R., Dickinson H.G., Boutilier K., VandenBosch K.A., Ohki S., Gutierrez-Marcos J.F. (2014): Centrall-cell derived peptides regulate early embryo patterning in flowering plants. *Science* **344**, 168-172.

Courgeon A. M., Maisonhaute C., Best-Belpomme M. (1984): Heat shock proteins are induced by cadmium in Drosophila cells. *Experimental Cell Research* **153**, 515-521.

Czar M. J., Galigniana M. D., Silverstein A. M., Pratt W. B. (1999): Geldanamycin, a heat shock protein 90-binding benzoquinone ansamysin, inhibits steroid-dependent translocation of the glucocorticoid receptor from the cytoplasm to the nucleus. *Biochemistry* **36**, 7776–7785.

Dickinson P.J., Kumar M., Martinho C., Yoo S.J., Lan H., Artavanis G., Charoensawan V., Schöttler M.A., Bock R., Jaeger K.E., Wigge P.A. (2018): Chloroplast Signaling Gates Thermotolerance in *Arabidopsis*. *Cell Reports* **22**, 1657–1665.

Feder M.E., Hofmann G.E. (1999): Heat-shock proteins, molecular chaperones, and stress response: evolutionary and ecological physiology. *Annual Review of Physiology* **61**, 243-282.

Franke J., Eichner S., Zeilinger C., Kirschning A. (2013): Targeting heat-shock-protein 90 (Hsp90) by natural products: geldanamycin, a show case in cancer therapy. Natural Product Report 30, 1299-1323.

GABI-Kat: https://www.gabi-kat.de/ 11.9.2018

Gudesblat G.E., Schneider-Pizón J., Betti C., Mayerhofer J., Vanhoutte I., et al. (2012): SPEECH-LESS integrates brassinosteroid and stomata signalling pathways. *Nature Cell Biology* **14**, 548–554.

Hartl F.U. (1996): Molecular chaperones in cellular protein folding. *Nature* **381**, 571-579.

Holt S. E., Aisner D. L., Baur J., Tesmer V. M., Dy M., Ouellette M., Trager J. B., Morun G. B., Toft D. O., Shay J. W., Wright W. E., White M. A. (1999): Functional requirement of p23 and Hsp90 in telomerase complexes. *Genes and Development* **13**, 817–826.

Hu W., Hu G., Han B. (2009): Genome-wide survey and expression profiling of heat shock proteins and heat shock factors revealed overlapped and stress specific response under abiotic stresses in rice. *Plant Science* **176,** 583-590.

Huang J. B., Liu H., Chen M., Li X., Wang M., Yang Y., Wang C., Huang J., Liu G., Liu Y., Xu J., Cheung A., Y., Tao L. Z. (2014): ROP3 GTPase Contributes to Polar Auxin Transport and Auxin Responses and Is Important for Embryogenesis and Seedling Growth in *Arabidopsis*. *Plant Cell* (http://www.plantcell.org/content/early/2014/09/09/tpc.114.127902.short)

Huang Y., Li H., Hutchinson CE., Laskey J., Kieber JJ. (2003): Biochemical and functional analysis of CTR1, a protein kinase that negatively regulates ethylene signaling in Arabidopsis. *The Plant Journal* **33**, 221-233.

Cha J. Y., Ahn G., Kim J. Y., Kang S. B., Kim M. R., Su'udi M., Kim W. Y., Son D. (2013): Structural and functional differences of cytosolic 90-kDa heat-shock proteins (Hsp90s) in Arabidopsis thaliana. *Plant Psychology and Biochemistry* **70**, 368-373.

Ichimura K., Mizoguchi T., Yoshida R., Yuasa T., Schinozaki K. (2000): Various abiotic stresses rapidly activate *Arabidopsis* MAP kinase AtMPK4 and AtMPK6. *Plant Journal* **24**, 655-665.

Ichimura K., Schinozaki K., Tena G, Sheen J., Henry Y., Champion A., Kreis M., Zhang S., Hirt H., Wilson C., Heberle-Bors E., Ellis B.E., Morris P.C., Innes R.W., Ecker J.R., Scheel D., Klessig D.F., Machida Y., Mundy J., Ohashi Y., Walker J.C. (2002): Mitogen-activated protein kinase cascades in plants: a vew nomenclature. *Trends in Planc Science* **7**, 301-308.

Jeong S., Eilbert E., Bolbol A., Lukowinz W. (2016): Going mainstream: How is the body axis of plants first initiated in the Embryo? Developmental Biology 419, 78-84.

Johnson B. D., Schumacher R. J., Ross E. D., Toft D. O. (1998):Hop modulates Hsp70/Hsp90interactions in protein folding. *Journal of Biological Chemistry* **273,** 3679–3686.

Kadota Y., Shirasu K. (2012): The HSP90 complex of plants. *Biochemica et Biophysica Act*a **1823**, 689-697.

Kampinga H.H., Craig E.A., (2010): The HSP70 chaperone machinery: J proteins as drivers of functional specificity. *Nature Reviews Molecular Cell Biology* **11**, 579–592.

Kaufman B.A., Kolesar J.E., Perlman P.S., Butow R.A. (2003): A function for the mitochondrial chaperonin Hsp60 in the structure and transmission of mitochondrial DNA nucleoids in *Saccharomyces cerevisiae*. *Journal of Cell Biology* **163**, 457-461.

Kaufman B.A., Newman S.M., Hallberg R.L., Slaughter C.A., Perlman P.S., Butow R.A. (2000): In organello formaldehyde crosslinking of proteins to mtDNA: identification of bifunctional proteins. *Proceedings of the National Academy of Sciences of the United States of America* **97**, 7772-7777.

Kirchhoff S.R., Gupta S., Knowlton A.A. (2002): Cytosolic heat shock protein 60, apoptosis, and myocardial injury. *Circulation* **105**, 2899-2904.

Kodíček M, Valentová O., Hynek R. (2018): Enzymy – katalyzátory chemických reakcí. In: Biochemie - chemický pohled na biologický svět.2vydání VŠCHT Praha. 113.

Komis G., Šamajová O., Ovečka M., Šamaj J**.** (2018) Cell and developmental biology of plant mitogen-activated protein kinases. Annual Review of Plant Biology 69, 237-265.

Kotak S., Larkindale J., Lee U., Von Koskull-Döring P., Vierling E., Scharf K.D. (2007): Complexity of the heat stress response in plants. *Current Opinion in Plant Biology* **10**, 310-316.

Kotvun Y., Chiu W.L., Tena G., Sheen J. (2000): Functional analysis of oxidative stress-activated mitogen-activated protein kinase cascade in plants. **97**, 2940-2945.

Krishna P., Gloor G. (2001): The Hsp90 family of proteins in *Arabidopsis thaliana. Cell Stress and Chaperones*. **6**, 238-246.

Larkindale J., Hall J.D., Knight M.R., Vierling E. (2005): Heat stress phenotypes of *Arabidopsis* mutants implicate multiple signaling pathways in the acquisition of thermotolerance. *Plant Physiology* **138**, 882-897.

Lau S., Slane D., Herud O., Kong J., Jürgens G. (2012): Early Embryogenesis in Flowering Plants: Setting Up the Basic Body Pattern. *Annual Review of Plant Biology* **63**, 483–506.

Ludwig-Muller J, Krishna P, Forreiter C. 2000. A glucosinolate mutant of Arabidopsis is thermosensitive and defective in cytosolic hsp90 expression after heat stress. *Plant Physiology* **123**, 949–958.

Lukowitz W., Roeder A., Parmenter D., Somerville C. (2004): A MAPKK kinase gene regulates extra-embryonic cell fate on Arabidopsis. *Cell* **116**, 109-119.

Lukowitz W., Roeder A., Parmenter D., Somerville C. (2004): A MAPKK kinase gene regulates extra-embryonic cell fate on *Arabidopsis. Cell* **116**, 109-119.

Ma L, Gao Y, Chen Z, Li J, Zhao H, Deng XW. 2002. Genomic evidence for COP1 as a repressor of light-regulated gene expression and development in Arabidopsis. The Plant *Cell* **14**, 2383– 2398.

Mashaghi A., Bezrukavnikov S., Minde D.P., Wentink A.S., Kityk R., Zachmann-Brand B., Mayer M.P., Kramer G., Bukau B., Tans S.J. (2016): Alternative modes of client binding enable functional plasticity of Hsp70. *Nature* **539**, 448-453.

Mason C.A., Dunner J., Indra P., Colangelo T. (1999): Heat-induced expression and chemically induced expression of the *Escherichia coli* stress protein HtpG are affected by the growth environment. *Applied and Environmental Microbiology* **65**, 3433–3440.

Mayerowitz E. M. (2001): Prehistory and History of Arabidopsis Research. *Plant Physiology* **125**, 15-19.

Meister M., Tomasovic A., Banning A., Tikkanen R. (2013): Mitogen-Activated Protein (MAP) Kinase Scaffolding Proteins: A Recount. *International Journal of Molecular Sciences* **14**, 4854-4884.

Meng X., Wang H, He Y,. Liu Y., Walker J.C., Torii K.U., Zhang S. (2012): A MAPK cascade downstream of ERECTA reseptor-like protein kinase regulates *Arabidopsis* influorescence architecture by promoting localized cell proliferation. *The Plant Cell* **24**, 4948-4960.

Meng X., Wang H., He Y., Liu Y., Walker J. C., Torii K. U., Zhang S. (2012): A MAPK cascade downstream of ERECTA receptor-like protein kinase regulates *Arabidopsis* inflorescence architecture by promoting localized cell proliferation. *The Plant Ce*ll **24**, 4948-4960.

Milioni D., Hatzopoulos P. (1997): Genomic organization of hsp90 gene family in *Arabidopsis*. *Plant Molecular Biology* **35**, 955–961.

Müller S. (2012): Plant Cell Division. *eLS. John Wiley & Sons* https://doi.org/10.1002/9780470015902.a0023760 (10.09.2018)

Panaretou B., Prodromou C., Roe S.M., O'Brien R., Ladbury J.E., Piper P.W., Pearl L.H. (1998): ATP binding and hydrolysis are essential to the function of the Hsp90 molecular chaperone *in vivo*. The *EMBO Journal* **17**, 4829–4836.

Panaretou B., Zhai C. (2008): The heat shock proteins: their roles as multi-component machines for protein folding. *Fungal biology reviews* **22**, 110-119.

Pearl L.H., Prodromou C. (2000): Structure and in vivo function of Hsp90. *Current Opinion in Structural Biology* **10**, 46–51.

Peris C. I. L., Rademacher E. H., Weijers D. (2010): Green Beginnings — Pattern Formation in the Early Plant Embryo. *Current Topics in Developmental Biology* **91,** 1-27.

Petersen M., Brodersen P., Naested H., Andreasson E., Lindhart U., Johansen B., Nielsen H. B., Lacy M., Austin M. J., Parker J. E., Sharma S. B., Klessig D. F., Martienssen R., Mattsson O., Jensen A. B., Mundy J. (2000): Arabidopsis map kinase 4 negativelyregulates systemic acquired resistance. **Cell** *103*, 1111-1120.

Pratt W. B., Krishna P., Olsen L. J. (2001): Hsp90-binding immunophilins in plants: the protein movers. *Trends in Plant Science* **6**, 54–58.

Ritossa F. (1962): A new puffing pattern induced by heat shock and DNP in Drosophila. *Experientia*. **18**, 571–573.

Rizhsky L., Liang H., Mittler R. (2002): The Combined Effect of Drought Stress and Heat Shock on Gene Expression in Tobacco. *Plant Physiology* **130**, 1143-1151.

Rodriguez MC, Peterson M, Mundy J. (2010): Mitogen-activated protein kinase signaling in plants. *Annual Review of Plant Biology* **61**, 621-649.

Rutherford SL, Lindquist S. 1998. Hsp90 as a capacitor for morphological evolution. *Nature* **396**, 336–342.

Samakovli D., Thanou A., Valmas C., Hatzopulos P. (2007): HSP90 canalizes developmental perturbation. Journal of experimental botany 58, 3513-3524.

Sangster T. A., Lindquist S., Queitsch C. (2004): Under cover: causes, effects and implications of Hsp90-mediated genetic capacitance. *BioEssays* **26**, 348–362.

Sharma S.K., De los Rios P., Christen P., Lustig A., Goloubinoff P. (2010): The kinetic parameters and energy cost of the Hsp70 chaperone as a polypeptide unfoldase. *Nature Chemical Biology* **6**, 914–920.

Scharf K.D., Siddique M., Vierling E. (2001): The expanding family of Arabidopsis thaliana small heat stress proteins and a new family of proteins containing alpha-crystallin domains (Acd proteins). *Cell Stress Chaperones* **6**, 225–237.

Schlesinger M.J. (1990): Heat shock proteins. *Journal of Biological Chemistry* **265**, 12111-12114.

Smékalová V., Luptovčiak I., Komis G., Šamajová O., Ovečka M., Doskočilová A., Takáč T., Vadovič P., Novák O., Pechan T., Ziemann A., Košútová P., Šamaj J. (2014): Involvement of YODA and mitogen activated protein kinase 6 in Arabidopsis post-embryogenic root development through auxin up-regulation and cell division plane orientation. *New Physiology* **203**, 1175-1193.

Sorger P.K., Nelson H.C. (1989): Trimerization of a yeast transcriptional activator via a coiled-coil motif. *Cell* **59**, 807-813.

Sun W., Bernard C., Van De Cotte B., Van Montagu M., Verbruggen N. (2001): At-HSP17.6A, encoding a small heat-shock protein in Arabidopsis, can enhance osmotolerance upon overexpression. *The Plant Journal* **27**, 407-415.

Šamajová O., Plíhal O., Al-Yousif M., Hirt H., Šamaj J. (2013): Improvement of stress tolerance in plants by genetic manipulation of mitogen-activated protein kinases. *Biotechnology Advances* **31**, 118-128.

TAIR: https://www.arabidopsis.org/portals/education/aboutarabidopsis.jsp (27.8.2018)

Takahashi Y., Soyano T., Kosetsu K., Sasabe M., Machida Y. (2010): HINKEL kinesin, ANP MAPKKKs and MKK6/ANQ MAPKK, which phosphorylates and activates MPK4 MAPK, constitute a pathway that is required for cytokinesis in Arabidopsis thaliana. *Plant and Cell Physiology* **51**, 1766-1776.

Teige M, Scheikl E, Eulgem T, Doczi R, Ichimura K, et al. 2004. The MKK2 pathway mediates cold and salt stress signaling in Arabidopsis. *MolecularCell* **15**, 141–52.

ten Hove C. A., Lu K. J., Weijers D. (2015): Building a plant: cell fate specification in the early *Arabidopsis* embryo. *Development* **142**, 420-430.

Tissieres A., Mitchell H.K., Tracy U.M. (1974): Protein synthesis in salivary glands of Drosophila melanogaster: Relation to chromosome puffs. *Journal of Molecular Biology* **85**, 389-398.

Truernit E., Bauby H., Dubreucq B., Grandjean O., Runions J., Barthelémy J., Palauqui J., C. (2008): High-Resolution Whole-Mount Imaging of Three-Dimensional Tissue Organization and Gene Expression Enables the Study of Phloem Development and Structure in *Arabidopsis*. *Plant Cell* **20**, 1494-1503.

Ueda M., Aichinger E., Gong W., Groot E., Verstraeten I., Vu L. D., De Smet I., Higashiyama T., Umeda M., Laux T. (2017): Transcriptional integration of paternal and maternal factors in the *Arabidopsis zygote*. *Genes & Development* **31**, 617–627.

Ueda M., Zhang Z., Laux T. (2011): Transcriptional activation of *Arabidopsis* axis patterning genes WOX8/9 links zygote polarity to embryo development. *Developmental Cell* **20**, 264-270.

Virk N, Li D., Tian L., Huang L., Hong Y., Li X., Zhang Y., Liu B., Zhang H. (2015): *Arabidopsis* Raf-like Mitogen-Activated Protein Kinase Kinase Gene Raf43 Is Required for Tolerance to Multiple Abiotic Stresses, *PLOS Genetics* ttps://doi.org/10.1371/journal.pone.0133975

Wang H., Ngwenyama N., Liu Y., Walker J.C., Zhang S. (2007): Stomatal development and patterning are regulated by environmentally responsive mitogen-activated protein kinases in *Arabidopsis*. *Plant cell* **19**, 63-73.

Waters E. R. (2013): The evolution, function, structure, and expression of the plant sHSPs. *Journal of Experimental Botany* **64**, 391-403.

Xu X., Song H., Zhou Z., Shi N., Ying Q., Wang H. (2010): Functional characterization of AtHsp90.3 in *Saccharomyces cerevisiae* and *Arabidopsis thaliana* under heat stress. *Biotechnology Letters* **32**, 979–987.

Zhao C., Nie H., Shen Q., Zhang S., Lupkowitz W., Tang D. (2014): EDR1 Physically Interacts with MKK4/MKK5 and Negatively Regulates a MAP Kinase Cascade to Modulate Plant Innate Immunity**.** *PLOS Genetics* https://doi.org/10.1371/journal.pgen.1004389

Zhao R., Davey M., Hsu Y.C., Kaplanek P., Tong A., Parsons A.B., Krogan N., Cagney G., Mai D., Greenblatt J., Boone C., Emili A., Houry W.A. (2004): Navigating the Chaperone Network: An Integrative Map of Physical and Genetic Interactions Mediated by the Hsp90 Chaperone. *Cell* **120**, 715-727.

7 List of abbreviations

ANP kinase family	*Arabidopsis* homologue of Nucleus and Phragmoplast localized
Apaf1	Apoptotic protease activating factor 1
CTD	C-terminal domain
CTR1	CONSTITUTIVE TRIPLE RESPONSE
EDR1	ENHANCED DISEASE RESISTANCE 1
ESFs	EMBRYO SURROUNDING FACTORS
HDG	HOMEODOMAIN GLABROUS
HSE	Heat shock element
HSF	Heat shock factor
HSPs	Heat shock proteins
MAPKKKs	Mitogen activated protein kinase kinase kinase
MAPKKs	Mitogen activated protein kinase kinase
MAPKs	Mitogen activated protein kinases
MD	Middle domain
MEKK1	Mammalian MAP/ERK kinase kinase 1
NTD	N-terminal domain
RAF-like kinases	Rapidly accelerated fibrosarcoma
ROP	RHO GTPase OF PLANT
SPCH	SPEECHLESS
SSP	SHORT SUSPENSOR
WOX8	WUSCHEL HOMEOBOX 8
WRKY2	*Arabidopsis thaliana* WRKY DNA-binding factor 2